Graph Neural Networks with Local Graph Parameters

Pablo Barceló[1,2], **Floris Geerts**[3], **Juan Reutter**[1,2], **Maksimilian Ryschkov**[3]
[1] Department of Computer Science, PUC, Chile
[2] Millennium Institute for Foundational Research on Data, Chile
[3] Department of Computer Science, University of Antwerp, Belgium
[pbarcelo,jreutter]@ing.puc.cl, [floris.geerts,maksimilian.ryschkov]@uantwerpen.be

Abstract

Various recent proposals increase the distinguishing power of Graph Neural Networks (GNNs) by propagating features between k-tuples of vertices. The distinguishing power of these "higher-order" GNNs is known to be bounded by the k-dimensional Weisfeiler-Leman (WL) test, yet their $\mathcal{O}(n^k)$ memory requirements limit their applicability. Other proposals infuse GNNs with local higher-order graph structural information from the start, hereby inheriting the desirable $\mathcal{O}(n)$ memory requirement from GNNs at the cost of a one-time, possibly non-linear, preprocessing step. We propose local graph parameter enabled GNNs as a framework for studying the latter kind of approaches. We precisely characterize their distinguishing power, in terms of a variant of the WL test, and in terms of the graph structural properties that they can take into account. Local graph parameters can be added to any GNN architecture, and are cheap to compute. In terms of expressive power, our proposal lies in the middle of GNNs and their higher-order counterparts. Further, we propose several techniques to aid in choosing the right local graph parameters. Our results connect GNNs with deep results in finite model theory and finite variable logics. Our experimental evaluation shows that adding local graph parameters often has a positive effect on a variety of GNNs, datasets and graph learning tasks.

1 Introduction

Context. Graph neural networks (GNNs) [Merkwirth and Lengauer, 2005, Scarselli et al., 2009], and its important class of Message Passing Neural Networks (MPNNs) [Gilmer et al., 2017], are one of the most popular methods for graph learning tasks. Such MPNNs use an iterative message passing scheme, based on the adjacency structure of the underlying graph, to compute vertex (and graph) embeddings in some real Euclidean space.

The expressive (or distinguishing) power of MPNNs is, however, rather limited [Morris et al., 2019, Xu et al., 2019]. Indeed, MPNNs will always identically embed two vertices (graphs) when these vertices (graphs) cannot be distinguished by the one-dimensional Weisfeiler-Leman (WL) algorithm. Two graphs G_1 and H_1 and vertices v and w that cannot be distinguished by WL (and thus any MPNN) are shown in Fig. 1. The expressive power of WL is well-understood [Cai et al., 1992, Dell et al., 2018, Arvind et al., 2020] and basically can only use *tree-based* structural information in the graphs to distinguish vertices. Hence, no MPNN can detect that vertex v in Fig. 1 is part of a 3-clique, whereas w is not. Similarly, MPNNs cannot detect that w is part of a 4-cycle, whereas v is not. Further limitations of WL in terms of graph properties can be found, e.g., in Arvind et al. [2020], Chen et al. [2020] and Tahmasebi and Jegelka [2020].

To remedy the weak expressive power of MPNNs, so-called *higher-order* MPNNs were proposed [Maron et al., 2019a, Morris et al., 2019, 2020], whose expressive power is well-understood and

35th Conference on Neural Information Processing Systems (NeurIPS 2021).

measured in terms of the k-dimensional WL procedures (k-WL) [Maron et al., 2019a, Chen et al., 2019a, Geerts, 2020, Sato, 2020, Azizian and Lelarge, 2021]. In a nutshell, k-WL operates on k-tuples of vertices and allows to distinguish vertices (graphs) based on structural information related to *graphs of treewidth* k [Dvorak, 2010, Dell et al., 2018]. By definition, WL = 1-WL. As an example, 2-WL can detect that vertex v in Fig. 1 belongs to a 3-clique or a 4-cycle since both have treewidth two. While more expressive than WL, the GNNs based on k-WL require $\mathcal{O}(n^k)$ operations in *each iteration*, where n is the number of vertices, hereby hampering their applicability.

A more practical approach is to extend the expressive power of MPNNs *whilst preserving their* $\mathcal{O}(n)$ *cost in each iteration*. Various such extensions [Kipf and Welling, 2017, Chen et al., 2019a, Li et al., 2019, Ishiguro et al., 2020, Bouritsas et al., 2020, Geerts et al., 2021] achieve this by infusing MPNNs with *local graph structural information from the start*. That is, the iterative message passing scheme of MPNNs is run on vertex labels that contain quantitative information about local graph structures.

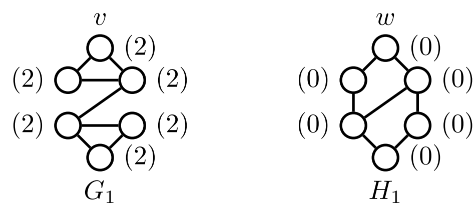

Figure 1: Two graphs that are indistinguishable by the WL-test. The numbers between round brackets indicate how many homomorphic images of the 3-clique each vertex is involved in.

It is easy to see that such architectures can go beyond the WL test: for example, adding triangle counts to MPNNs suffices to distinguish the vertices v and w and graphs G_1 and H_1 in Fig. 1. Moreover, the cost is *a single preprocessing step* to count local graph parameters, thus maintaining the $\mathcal{O}(n)$ cost in the iterations of the MPNN. While there are some partial results showing that local graph parameters increase expressive power [Bouritsas et al., 2020, Li et al., 2019], their precise expressive power and relationship to higher-order MPNNs was unknown, and there is little guidance in terms of which local parameters do help MPNNs and which ones do not. The main contribution of this paper is a precise characterization of the expressive power of MPNNs with local graph parameters and its relationship to the hierarchy of higher-order MPNNs.

Our contributions. In order to nicely formalize local graph parameters, we propose to extend vertex labels with *homomorphism counts* of small graph patterns.[1] More precisely, given graphs P and G, and vertices r in P and v in G, we propose to augment the initial features of v with the number of homomorphisms from P to G that map r to v, denoted by $\mathsf{hom}(P^r, G^v)$, as a way to capture local structural information. More generally, homomorphism counts for a collection of graphs are considered. Indeed, we propose $\mathcal{F}$-MPNNs where $\mathcal{F} = \{P_1^r, \ldots, P_\ell^r\}$ is a set of (graph) patterns, which extend MPNNs by (i) first allowing a preprocessing step that labels each vertex v of a graph G with the vector $\big(\mathsf{hom}(P_1^r, G^v), \ldots, \mathsf{hom}(P_\ell^r, G^v)\big)$, and (ii) then run an MPNN on this labelling. Our main contributions are the following:

1. We precisely characterize the expressive power of $\mathcal{F}$-MPNNs by means of an extension of WL, denoted by $\mathcal{F}$-WL. This characterization gracefully extends the characterization for standard MPNNs, mentioned earlier, by setting $\mathcal{F} = \emptyset$, and provides insights in the expressive power of existing MPNN extensions, most notably the Graph Substructure Networks of Bouritsas et al. [2020].

2. We compare $\mathcal{F}$-MPNNs to higher-order MPNNs, which are characterized in terms of the k-WL-test. On the one hand, while $\mathcal{F}$-MPNNs strictly increase the expressive power of the WL-test, for any finite set $\mathcal{F}$ of patterns, 2-WL can distinguish graphs which $\mathcal{F}$-MPNNs cannot. On the other hand, for each $k \geq 1$ there are patterns P such that $\{P\}$-MPNNs can distinguish graphs which k-WL cannot.

3. We deal with the challenging problem of pattern selection and comparing $\mathcal{F}$-MPNNs based on the patterns included in $\mathcal{F}$. We prove two partial results: one establishing when a pattern P in $\mathcal{F}$ is redundant, and another result indicating when P does add expressive power, based on the treewidth of P compared to the treewidth of other patterns in $\mathcal{F}$.

4. Our theoretical results are complemented by an experimental study in which we show that for various GNN architectures, datasets and graph learning tasks, all part of the recent benchmark by Dwivedi et al. [2020], the augmentation of initial features with homomorphism counts of graph patterns has often a positive effect, and the cost for computing these counts incurs little to no overhead.

[1] We recall that homomorphisms are edge-preserving mappings between the vertex sets.

As such, we believe that $\mathcal{F}$-MPNNs not only provide an elegant theoretical framework for understanding local graph parameter enabled MPNNs, they are also a valuable alternative to higher-order MPNNs as a way to increase the expressive power of MPNNs. In addition, and as will be explained in Section 2, $\mathcal{F}$-MPNNs provide a unifying framework for understanding the expressive power of several other existing extensions of MPNNs. Proofs of our results and further details on the relationship to existing approaches and experiments can be found in the supplementary material.

Related Work. Works related to the distinguishing power of the WL-test, MPNNs and their higher-order variants are cited throughout the paper. Beyond distinguishability, GNNs are analyzed in terms of universality and generalization properties [Maron et al., 2019b, Keriven and Peyré, 2019, Chen et al., 2019b, Garg et al., 2020, Azizian and Lelarge, 2021], local distributed algorithms [Sato et al., 2019, Loukas, 2020], randomness in features [Sato et al., 2021, Abboud et al., 2021] and using local context matrix features [Vignac et al., 2020]. Other extensions of GNNs are surveyed, e.g., in Wu et al. [2021], Zhou et al. [2018] and Chami et al. [2021]. Related are also the Graph Homomorphism Convolutions by NT and Maehara [2020] which apply SVMs directly on a homomorphism count representation of vertices. Finally, our approach is reminiscent of graph representations by means of graphlet kernels [Shervashidze et al., 2009], but then on the level of vertices.

Limitations of our approach. One of the limitations of $\mathcal{F}$-MPNNs is that their expressive power depends on the set $\mathcal{F}$ of patterns. Our work offers tools and guidelines to help in this search, but the best set of patterns must still be found by trial-and-error. However, as we show in Section 6, MPNNs almost always benefit from any set of additional features, assuming that the resulting model goes beyond the WL test. Cliques and cycles are two types of simple patterns that are guaranteed to extend the WL test, and indeed we show that striking gains can be obtained by simply adding these features to existing benchmarks. For simplicity of exposition we focus on vertex-labelled undirected graphs but all our results can be extended to edge-labelled directed graphs.

2 Local Graph Parameter Enabled MPNNs

We here introduce our MPNNs with local graph parameters. We first recall some graph concepts.

Graphs. We consider undirected vertex-labelled graphs $G = (V, E, \chi)$, with V the set of vertices, E the set of edges and χ a mapping assigning a label to each vertex in V. The set of neighbors of a vertex is denoted by $N_G(v) = \{u \in V \mid \{u, v\} \in E\}$. A *rooted graph* is a graph in which one of its vertices is declared as its root. We denote a rooted graph by G^v, where $v \in V$ is the root and depict them as graphs in which the root is a blackened vertex, such as e.g., 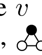. Given graphs $G = (V_G, E_G, \chi_G)$ and $H = (V_H, E_H, \chi_H)$, an *homomorphism* h is a mapping $h : V_G \to V_H$ such that (i) $\{h(u), h(v)\} \in E_H$ for every $\{u, v\} \in E_G$, and (ii) $\chi_G(u) = \chi_H(h(u))$ for every $u \in V_G$. For rooted graphs G^v and H^w, an homomorphism must additionally map v to w. We denote by $\mathsf{hom}(G, H)$ the number of homomorphisms from G to H; similarly for rooted graphs.

MPNNs with local graph parameters. Let $\mathcal{F} = \{P_1^r, \ldots, P_\ell^r\}$ be a set of rooted graphs, which we refer to as *patterns*. As a uniform formalization of local graph structural information, we propose the use of *homomorphism counts* of patterns in $\mathcal{F}$ to enhance the initial feature of vertices. To illustrate the idea, consider the graphs in Fig. 1. As mentioned, these graphs cannot be distinguished by the WL-test, and therefore cannot be distinguished by the broad class of MPNNs. If we allow a *preprocessing stage*, however, in which the initial labelling of every vertex v is extended with the number of (homomorphic images of) 3-cliques in which v participates (indicated by numbers between brackets in Fig. 1), then clearly vertices v and w (and the graphs G_1 and H_1) can be distinguished based on this extra structural information. In fact, the initial labelling already suffices for this purpose. In our setting, this will correspond to selecting the rooted 3-clique 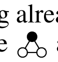 and attach to each vertex v, $\mathsf{hom}($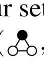$, G^v)$. Information about 4-cycles requires adding $\mathsf{hom}($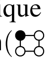$, G^v)$ as well.

We therefore propose $\mathcal{F}$*-enabled* MPNN*s*, or just $\mathcal{F}$-MPNNs, defined in the same way as MPNNs [Gilmer et al., 2017] with the crucial difference that the initial feature vector of a vertex v (a one-hot encoding of its label $\chi_G(v)$) is augmented with all the homomorphism counts from patterns in $\mathcal{F}$.

Formally, in each round d an $\mathcal{F}$-MPNN M labels each vertex v in graph G with a feature vector $\mathbf{x}_{M,\mathcal{F},G,v}^{(d)}$ which is inductively defined as follows:

$$\mathbf{x}^{(0)}_{M,\mathcal{F},G,v} := \big(\chi_G(v), \mathsf{hom}(P_1^r, G^v), \ldots, \mathsf{hom}(P_\ell^r, G^v)\big)$$
$$\mathbf{x}^{(d)}_{M,\mathcal{F},G,v} := \textsc{Upd}^{(d)}\Big(\mathbf{x}^{(d-1)}_{M,\mathcal{F},G,v}, \textsc{Comb}^{(d)}\big(\{\!\{\mathbf{x}^{(d-1)}_{M,\mathcal{F},G,u} \mid u \in N_G(v)\}\!\}\big)\Big), \text{ for } d > 0,$$

where $\textsc{Comb}^{(d)}$ and $\textsc{Upd}^{(d)}$ are an *aggregating* and *update* function, respectively, as in standard MPNNs, and where $\{\!\{\}\!\}$ denotes a multi-set. We note that standard MPNNs are $\mathcal{F}$-MPNNs with $\mathcal{F} = \emptyset$. As for MPNNs, we can equip $\mathcal{F}$-MPNNs with a $\textsc{Readout}$ function that aggregates all final feature vectors into a single feature vector in order to classify or distinguish graphs.

We remark that *any* MPNN architecture can be turned into an $\mathcal{F}$-MPNN by a simple homomorphism counting preprocessing step. As such, we propose a *generic plug-in for a large class of* GNN *architectures*. Better still, $\mathsf{hom}(P^r, G^v)$ can be computed in time $\mathcal{O}(|V_G|^{\mathsf{tw}(P^r)+1})$ [Díaz et al., 2002], where $\mathsf{tw}(P^r)$ denotes the treewidth of pattern P^r. The treewidth of patterns used in $\mathcal{F}$-MPNNs is typically small. And indeed, homomorphism counts of small graph patterns can be efficiently computed in practice, even on large datasets [Zhang et al., 2020]. We also remark that the use of rooted patterns is important because different vertices in a pattern may embed differently around a target vertex in a graph. For example, $\mathsf{hom}($$, G^v)$ can be different from $\mathsf{hom}($$, G^v)$. The choice of a root in a graph P can be avoided by including different rooted versions of P in $\mathcal{F}$. In fact, it suffices to include one rooted version P^r for each vertex r in a distinct orbit in P. We note that for symmetric graphs, such as cliques and cycles, all vertices lie in the same orbit and a single, arbitrary, choice of root vertex suffices. Alternatively, one could define $\mathsf{hom}(P, G^v) := \sum_{r \in V_P} \mathsf{hom}(P^r, G^v)$ which ignores how the pattern is locally mapped into a graph. We speculate, however, that this results in a model that is less powerful than $\mathcal{F}$-MPNNs.

Despite their simplicity, we will show that $\mathcal{F}$-MPNNs can substantially increase the power of MPNNs by varying $\mathcal{F}$, only paying a one-time preprocessing cost.

$\mathcal{F}$-MPNNs as unifying framework. An important aspect of $\mathcal{F}$-MPNNs is that they *allow a principled analysis of the power of existing extensions of* MPNN*s*. For example, taking $\mathcal{F} = \{$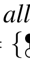$\}$ suffices to capture degree-aware MPNNs [Geerts et al., 2021], such as the Graph Convolution Networks (GCNs) [Kipf and Welling, 2017], which use the *degree of vertices*; taking $\mathcal{F} = \{L_1, L_2, \ldots, L_\ell\}$ for rooted paths L_i of length i suffices to model the *walk counts* used in Chen et al. [2019a]; and taking $\mathcal{F}$ as the set of labeled trees of depth one precisely corresponds to the use of the WL-*labelling obtained after one round* by Ishiguro et al. [2020]. Furthermore, $\{C_\ell\}$-MPNNs, where C_ℓ denotes the cycle of length ℓ, correspond to the extension proposed in Section 4 in Li et al. [2019].

In addition, $\mathcal{F}$-MPNNs are close in spirit to the *Graph Substructure Networks* (GSNs) by Bouritsas et al. [2020], which use subgraph isomorphism counts of graph patterns. We recall that an isomorphism from G to H is a *bijective* homomorphism h from G to H which additionally satisfies (i) $\{h^{-1}(u), h^{-1}(v)\} \in E_G$ for every $\{u, v\} \in E_H$, and (ii) $\chi_G(h^{-1}(u)) = \chi_H(u)$ for every $u \in V_H$. When G and H are rooted graphs, isomorphisms should preserve the roots as well. Now, in a GSN, the feature vector of each vertex v is augmented with the subgraph isomorphism counts, $\mathsf{sub}(P^r, G^v)$, for rooted patterns P^r in a set of $\mathcal{P}$ of patterns, and this is followed by the execution of an MPNN, just as for our $\mathcal{F}$-MPNNs. Importantly, $\mathcal{F}$-MPNNs can be used to bound the expressive power of GSNs, as we will show later. We note that computing $\mathsf{sub}(P^r, G^v)$ is, in general, more costly than computing $\mathsf{hom}(P^r, G^v)$ [Curticapean et al., 2017]. This partially motivates our choice of using homomorphism counts instead of subgraph isomorphism counts. Moreover, homomorphism counts of tree patterns underly existing characterizations of the expressive power of MPNNs [Dell et al., 2018, Grohe, 2020a]. As we will see shortly, these characterizations gracefully extend to $\mathcal{F}$-MPNNs.

3 The Expressive Power of $\mathcal{F}$-MPNNs

We next provide exact characterizations of the expressive power of $\mathcal{F}$-MPNNs. Our results extend those for standard MPNNs [Xu et al., 2019, Morris et al., 2019, Dell et al., 2018].

Characterization in terms of $\mathcal{F}$-WL. We bound the expressive power of $\mathcal{F}$-MPNNs in terms of what we call the $\mathcal{F}$-WL-*test*. This test extends the WL-test [Weisfeiler and Lehman, 1968, Grohe, 2017] in the same way as $\mathcal{F}$-MPNNs extend standard MPNNs: by including homomorphism counts of patterns in $\mathcal{F}$ in the initial labelling. The $\mathcal{F}$-WL-test, for $\mathcal{F} = \{P_1^r, \ldots, P_\ell^r\}$, is a vertex labelling algorithm that iteratively computes a label $\chi_{\mathcal{F},G,v}^{(d)}$ for each vertex v of a graph G, as follows:

$$\chi_{\mathcal{F},G,v}^{(0)} := \big(\chi_G(v), \mathsf{hom}(P_1^r, G^v), \ldots, \mathsf{hom}(P_\ell^r, G^v)\big)$$
$$\chi_{\mathcal{F},G,v}^{(d)} := \textsc{Hash}\big(\chi_{\mathcal{F},G,v}^{(d-1)}, \{\!\{\chi_{\mathcal{F},G,u}^{(d-1)} \mid u \in N_G(v)\}\!\}\big), \text{ for } d > 0.$$

The $\mathcal{F}$-WL-test stops in round d when no new pair of vertices are distinguished, that is, $\chi_{\mathcal{F},G,v_1}^{(d-1)} = \chi_{\mathcal{F},G,v_2}^{(d-1)}$ implies $\chi_{\mathcal{F},G,v_1}^{(d)} = \chi_{\mathcal{F},G,v_2}^{(d)}$, for any vertices v_1 and v_2 in G. The standard WL-test corresponds to $\{\emptyset\}$-WL. We can use the $\mathcal{F}$-WL-test to compare vertices of the same graphs, or different graphs. We say that the $\mathcal{F}$-WL-test *cannot distinguish vertices* if their final labels are the same, and that the $\mathcal{F}$-WL-test *cannot distinguish graphs* G and H if the multiset containing each label computed for G is the same as that of H. Similarly as for MPNNs and the WL-test [Xu et al., 2019, Morris et al., 2019], the $\mathcal{F}$-WL-test provides an upper bound for the expressiveness of $\mathcal{F}$-MPNNs.

Proposition 1. *If two vertices of a graph cannot be distinguished by the $\mathcal{F}$-WL-test, then they cannot be distinguished by any $\mathcal{F}$-MPNN either. Moreover, if two graphs cannot be distinguished by the $\mathcal{F}$-WL-test, then they cannot be distinguished by any $\mathcal{F}$-MPNN either.*

Furthermore, simply adding local parameters from a set $\mathcal{F}$ of patterns to the GIN architecture of Xu et al. [2019] results in $\mathcal{F}$-MPNNs that match the expressive power of the $\mathcal{F}$-WL-test.

Characterization in terms of $\mathcal{F}$-pattern trees. At the core of several results about the WL-test lies a characterization linking the test with homomorphism counts of (rooted) trees [Dell et al., 2018, Grohe, 2020a]. In view of the connection to MPNNs, it tells that MPNNs only use *quantitative tree-based* structural information from the underlying graphs. We next extend this characterization to $\mathcal{F}$-WL by using homomorphism counts of so-called *$\mathcal{F}$-pattern trees*. Proposition 1 then reveals that $\mathcal{F}$-MPNNs can use quantitative information of *richer graph structures* than the trees used by MPNNs.

To define $\mathcal{F}$-pattern trees we need the *graph join operator* $\star$. Given two rooted graphs G^v and H^w, the join graph $(G \star H)^v$ is obtained by taking the disjoint union of G^v and H^w, followed by identifying w with v. The root of the join graph is v. For example, the join of 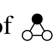 and 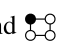 is 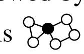. Furthermore, if G is a graph and P^r is a rooted graph, then joining a vertex v in G with P^r results in the disjoint union of G and P^r, where r is identified with v. Let $\mathcal{F} = \{P_1^r, \ldots, P_\ell^r\}$. An *$\mathcal{F}$-pattern tree* T^r is obtained from a standard rooted tree $S^r = (V, E, \chi)$, called the *backbone* of T^r, followed by joining every vertex $s \in V$ with any number of copies of patterns from $\mathcal{F}$. Examples of $\mathcal{F}$-pattern trees, for $\mathcal{F} = \{$$\}$ are shown in Fig. 2, where grey colored vertices are part of the backbones of the $\mathcal{F}$-pattern trees. We define the *depth* of an $\mathcal{F}$-pattern tree as the depth of its backbone. Standard trees are $\mathcal{F}$-pattern trees in which no patterns are joined with backbone vertices. We next use $\mathcal{F}$-pattern trees to characterize the expressive power of $\mathcal{F}$-WL and thus, by Proposition 1, of $\mathcal{F}$-MPNNs.

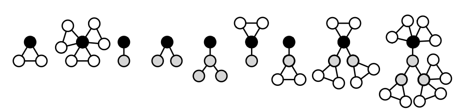

Figure 2: Examples of $\mathcal{F}$-pattern trees.

Theorem 1. *For any finite collection $\mathcal{F}$ of patterns, vertices v and w in a graph G are indistinguishable by the $\mathcal{F}$-WL-test if and only if $\mathsf{hom}(T^r, G^v) = \mathsf{hom}(T^r, G^w)$ for every rooted $\mathcal{F}$-pattern tree T^r. Similarly, G and H are indistinguishable by the $\mathcal{F}$-WL-test if and only if $\mathsf{hom}(T, G) = \mathsf{hom}(T, H)$ for every (unrooted) $\mathcal{F}$-pattern tree T.*

The proof of this Theorem requires a generalization of the techniques from Dell et al. [2018] and Grohe [2020a,b], used to characterize the expressiveness of WL in terms of homomorphism counts of trees. In fact, we can use our proof to recover said results simply by setting $\mathcal{F} = \emptyset$. We note that $\mathcal{F}$-MPNNs are more expressive than MPNNs (recall the graphs G_1 and H_1 and $\mathcal{F} = \{$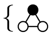$\}$).

We can even make the above theorem more precise. When $\mathcal{F}$-WL is run for d rounds, then *only $\mathcal{F}$-patterns trees of depth d are required*. This tells that increasing the number of rounds of $\mathcal{F}$-WL results in that more complicated structural information is taken into account. As an illustration, consider the graphs G_2 and H_2 and vertices v and w shown in Fig. 3 and let us consider $\mathcal{F}$-WL with $\mathcal{F} = \{$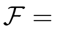$\}$. We argue that v and w cannot be distinguished by $\mathcal{F}$-WL based on the initial labelling only, but they can be distinguished after one round.

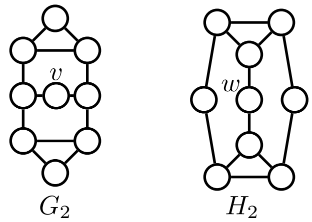

Figure 3: { }–MPNNs require one round to distinguish v from w.

Indeed, by definition, $\mathcal{F}$-WL cannot distinguish v from w based on the initial labelling since these vertices have the same triangle count (zero). Hence, no $\mathcal{F}$-MPNN can distinguish these vertices either. If run for one round, Theorem 1 implies that $\mathcal{F}$-WL cannot distinguish v from w if and only if $\mathsf{hom}(T^r, G_2^v) = \mathsf{hom}(T^r, H_2^w)$ for any $\mathcal{F}$-pattern tree of depth at most 1. It is readily verified that $\mathsf{hom}(\ , G_2^v) = 0 \neq 4 = \mathsf{hom}(\ , H_2^w)$, and thus $\mathcal{F}$-WL distinguishes v from w after one round. Also, G_2 and H_2 can be distinguished by $\mathcal{F}$-WL after one round. Moreover, G_2 and H_2 are indistinguishable by WL showing again that $\mathcal{F}$-MPNNs are more expressive than MPNNs. The example shows that more rounds allow $\mathcal{F}$-MPNNs to detect more complex patterns based on $\mathcal{F}$-pattern trees. This is in contrast to, e.g., the Graph Homomorphism Convolutions by NT and Maehara [2020] in which only homomorphism counts of patterns in $\mathcal{F}$, and not the counts of the derived $\mathcal{F}$-patterns trees, are taken into account.

Implications for other MPNN extensions. Importantly, Theorem 1 discloses the boundaries of $\mathcal{F}$-MPNNs. To illustrate this for some specific instances of $\mathcal{F}$-MPNNs mentioned earlier, the expressive power of degree-based MPNNs [Kipf and Welling, 2017, Geerts et al., 2021] is captured by $\{L_1\}$-pattern trees, and walk count MPNNs [Chen et al., 2019a] are captured by $\{L_1, \ldots, L_\ell\}$-pattern trees. These pattern trees are just trees, since joining paths to trees only results in bigger trees. Thus, Theorem 1 tells that all these extensions are still bounded by WL (albeit needing fewer rounds). In contrast, beyond WL, $\{C_\ell\}$-pattern trees capture cycle count MPNNs [Li et al., 2019]. Our results also shed light on the expressive power of GSNs [Bouritsas et al., 2020] which, as already mentioned, use subgraph isomorphism counts of patterns $P \in \mathcal{P}$. More precisely, a $\mathcal{P}$-GSN augments vertex features by including $\mathsf{sub}(P^r, G^v)$ for rooted versions P^r of $P \in \mathcal{P}$, where r ranges over representative vertices of the different orbits in P. Let us denote by $\mathcal{P}^+$ this set of rooted patterns.

Fact 1 (Curticapean et al. [2017])**.** *For any set $\mathcal{P}$ of rooted patterns, there exists a pattern set* $\mathsf{s}(\mathcal{P})$ *such that for each $P^r \in \mathcal{P}$,* $\mathsf{sub}(P^r, G^v)$ *can be computed based on* $\{\mathsf{hom}(Q^r, G^v) \mid Q^r \in \mathsf{s}(\mathcal{P})\}$.

In other words, subgraph isomorphism counts can be computed in terms of homomorphism counts, albeit by using different pattern sets. For example, if $\mathcal{P} = \{ \ \}$, then $\mathsf{s}(\mathcal{P}) = \{ \ , \ , \ , \ \}$ which contains all different homomorphic images of . As a consequence, we obtain:

Proposition 2. $\mathcal{P}$-GSN*s cannot distinguish more vertices than* $\mathsf{s}(\mathcal{P}^+)$-MPNN*s can.*

So, we can bound the expressive power of GSNs in terms of $\mathcal{F}$-MPNNs. In the supplementary material we also show that $\mathcal{F}$-MPNNs are bounded by GSNs that use some special set of patterns derived from $\mathcal{F}$. We conclude by observing that the proof technique underlying Theorem 1 can be directly applied to GSNs. The key insight is to redefine the notion of homomorphism from pattern trees to graphs. Indeed, consider a $\mathcal{P}$-GSN and a corresponding $\mathcal{P}^+$-pattern tree T^r. We define $\mathsf{shom}(T^r, G^v)$ as the number of mappings $h : V_T \to V_G$ such that (i) $h(r) = v$; (ii) h is a homomorphism when restricted to the backbone of T^r; and (iii) for each P^r joined with a backbone vertex, $h(P^r)$ is *isomorphic* to P^r. We then have the following counterpart of Theorem 1 for GSNs:

Theorem 2. *For any finite collection $\mathcal{P}$ of patterns, vertices v and w in a graph G are indistinguishable by $\mathcal{P}$-*GSN*s if and only if* $\mathsf{shom}(T^r, G^v) = \mathsf{shom}(T^r, G^w)$ *for every rooted $\mathcal{P}^+$-pattern tree T^r. Similarly, G and H are indistinguishable by $\mathcal{P}$-*GSN*s if and only if* $\mathsf{shom}(T, G) = \mathsf{shom}(T, H)$ *for every (unrooted) $\mathcal{P}^+$-pattern tree T.*

4 A Comparison with the k-WL-test

Compared to the computationally intensive higher-order MPNNs based on the k-WL-tests [Maron et al., 2019a, Morris et al., 2019, 2020], $\mathcal{F}$-MPNNs are an alternative and efficient way to extend the expressive power of MPNNs (and thus the WL-test). In this section we situate $\mathcal{F}$-WL in the k-WL hierarchy. The definition of the k-WL-test can be found, e.g., in Morris et al. [2020], and is provided in the supplementary material as well. We also use the standard notion of *treewidth* of a graph (see e.g., Bodlaender [1993]). Intuitively, treewidth measures the tree-likeness of a graph. For example, trees have treewidth one, cycles have treewidth two, and the k-clique K_k has treewidth $k - 1$. Furthermore, the treewidth of a pattern P^r is the treewidth of its unrooted version P.

We have seen that $\mathcal{F}$-WL can distinguish graphs that WL cannot: just consider $\{K_3\}$-WL for the 3-clique K_3. To generalize this observation we need some notation. Let $\mathcal{F}$ and $\mathcal{G}$ be two sets of patterns and consider an $\mathcal{F}$-MPNN M and a $\mathcal{G}$-MPNN N. We say that M is *upper bounded in expressive power* by N if for any graph G, if N cannot distinguish vertices v and w,[2] then neither can M. A similar notion is in place for pairs of graphs: if N cannot distinguish graphs G and H, then neither can M. More generally, let $\mathcal{M}$ be a class of $\mathcal{F}$-MPNNs and $\mathcal{N}$ be a class of $\mathcal{G}$-MPNNs. We say that the class $\mathcal{M}$ is *upper bounded in expressive power* by $\mathcal{N}$ if every $M \in \mathcal{M}$ is upper bounded in expressive power by an $N \in \mathcal{N}$ (which may depend on M). When $\mathcal{M}$ is upper bounded by $\mathcal{N}$ and vice versa, then $\mathcal{M}$ and $\mathcal{N}$ are said to have the *same expressive power*. A class $\mathcal{N}$ is *more expressive* than a class $\mathcal{M}$ when $\mathcal{M}$ is upper bounded in expressive power by $\mathcal{N}$, but there exist graphs that can be distinguished by MPNNs in $\mathcal{N}$ but not by any MPNN in $\mathcal{M}$.

Our first result is a consequence of the characterization of k-WL in terms of homomorphism counts of graphs of treewidth k [Dvorak, 2010, Dell et al., 2018].

Proposition 3. *For each finite set $\mathcal{F}$ of patterns, the expressive power of $\mathcal{F}$-WL is bounded by k-WL, where k is the largest treewidth of a pattern in $\mathcal{F}$.*

For example, since the treewidth of K_3 is 2, we have that $\{K_3\}$-WL is bounded by 2-WL. Similarly, $\{K_{k+1}\}$-WL is bounded in expressive power by k-WL.

Our second result tells how to increase the expressive power of $\mathcal{F}$-WL beyond k-WL. A pattern P^r is a *core* if any homomorphism from P to itself is injective. For example, any clique K_k and cycle of odd length is a core.

Theorem 3. *Let $\mathcal{F}$ be a finite set of patterns. If $\mathcal{F}$ contains a pattern P^r which is a core and has treewidth k, then there exist graphs that can be distinguished by $\mathcal{F}$-WL but not by $(k-1)$-WL.*

In other words, for such $\mathcal{F}$, $\mathcal{F}$-WL is not bounded by $(k-1)$-WL. For example, since K_3 is a core, $\{K_3\}$-WL is not bounded in expressive power by WL $=$ 1-WL. More generally, $\{K_k\}$-WL is not bounded by $(k-1)$-WL. The proof of Theorem 3 is based on extending deep techniques developed in finite model theory, and that have been used to understand the expressive power of *finite variable logics* [Atserias et al., 2007, Bova and Chen, 2019]. This result is stronger than the one underlying the strictness of the k-WL hierarchy [Otto, 2017], which states that k-WL is strictly more expressive than $(k-1)$-WL. Indeed, Otto [2017] only shows the *existence* of a pattern P^r of treewidth k such that $(k-1)$-WL is not bounded by $\{P^r\}$-WL. In Theorem 3 we provide an *explicit recipe* for finding such a pattern P^r, that is, P^r can be taken a core of treewidth k.

In summary, we have shown that there is a set $\mathcal{F}$ of patterns such that (i) $\mathcal{F}$-WL can distinguish graphs which cannot be distinguished by $(k-1)$-WL, yet (ii) $\mathcal{F}$-WL cannot distinguish more graphs than k-WL. This begs the question whether there is a finite set $\mathcal{F}$ such that $\mathcal{F}$-WL is equivalent in expressive power to k-WL. We answer this negatively.

Proposition 4. *For any $k > 1$, there does not exist a finite set $\mathcal{F}$ of patterns such that $\mathcal{F}$-WL is equivalent in expressive power to k-WL.*

In the proof of Proposition 4 we show a stronger claim. Indeed, we construct two graphs that can be distinguished by 2-WL but cannot be distinguished by any $\mathcal{F}$-WL. Since any two graphs that can be distinguished by 2-WL can also be distinguished by k-WL, for any $k > 2$, the proposition follows. In view of the connection between $\mathcal{F}$-MPNNs and GSNs mentioned earlier, we thus show that no GSN can match the power of k-WL, which was a question left open in Bouritsas et al. [2020]. We remark that if we allow $\mathcal{F}$ to consist of all (*infinitely many*) patterns of treewidth k, then $\mathcal{F}$-WL is equivalent in expressive power to k-WL [Dvorak, 2010, Dell et al., 2018].

5 When Do Patterns Extend Expressiveness?

Graph patterns are not learned, but must be passed as an input to MPNNs together with the graph structure. Thus, knowing which patterns work well, and which do not, is of *key importance for the power of the resulting $\mathcal{F}$-MPNNs*. This is a difficult question to answer since determining which patterns work well is clearly application-dependent. From a theoretical point of view, however, we can still look into interesting questions related to the problem of which patterns to choose. One such

[2] As for the $\mathcal{F}$-WL-test, $\mathcal{F}$-MPNNs cannot distinguish vertices if they are assigned the same feature vector.

a question, and the one studied in this section, is when a pattern adds expressive power over the ones that we have already selected. More formally, we study the following problem: *Given a finite set $\mathcal{F}$ of patterns, when does adding a new pattern P^r to $\mathcal{F}$ extends the expressive power of the $\mathcal{F}$-WL-test?*

To positively answer this question, we need to find two graphs G and H, show that they are indistinguishable by the $\mathcal{F}$-WL-test, but show that they can be distinguished by the $\mathcal{F} \cup \{P^r\}$-WL-test. As an example we show that longer cycles always add expressive power.

Proposition 5. *For any $\ell > 3$, $\{C_3^r, \ldots, C_\ell^r\}$-WL is more expressive than $\{C_3^r, \ldots, C_{\ell-1}^r\}$-WL.*

Here, C_ℓ denotes a cycle of length ℓ. We also observe that, by Proposition 3, $\{C_3^r, \ldots, C_\ell^r\}$-WL is bounded by 2-WL for any $\ell \geq 3$ because cycles have treewidth two.

In general, it is quite challenging to find two graphs and to prove that they are indistinguishable by $\mathcal{F}$-WL but can be distinguished by the $\mathcal{F} \cup \{P^r\}$-WL-test. Instead, in this section we provide two techniques that can be used to partially answer the question posed above by only looking at properties of the sets of patterns. Our first result is for establishing when a pattern does not add expressive power to a given set $\mathcal{F}$ of patterns, and the second one when it does.

Detecting when patterns are superfluous. Our first result states that instead of choosing complex patterns that are the joins of smaller patterns, one should opt for the smaller patterns.

Proposition 6. *Let $P^r = P_1^r \star P_2^r$ be a pattern that is the join of two smaller patterns. Then for any set $\mathcal{F}$ of patterns, we have that $\mathcal{F} \cup \{P^r\}$-WL is upper bounded by $\mathcal{F} \cup \{P_1^r, P_2^r\}$-WL.*

Stated differently, this means that adding to $\mathcal{F}$ any pattern which is the join of two patterns already in $\mathcal{F}$ does not add expressive power. For example, instead of the pattern 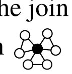 one should simply use the 3-clique . This is in line with other advantages of smaller patterns: their homomorphism counts are easier to compute, and, since they are less specific, they should tend to produce less over-fitting.

Detecting when patterns add expressiveness. Joining patterns into new patterns does not give extra expressive power, but what about patterns which are not joins? We next provide a useful recipe for detecting when a pattern does add expressive power. We recall that the *core of a graph P* is its unique (up to isomorphism) induced subgraph which is both a homomorphic image of P and a core.

Theorem 4. *Let $\mathcal{F}$ be a finite set of patterns and let Q^r be a pattern whose core has treewidth k. Then, $\mathcal{F} \cup \{Q^r\}$-WL is more expressive than $\mathcal{F}$-WL if every pattern $P^r \in \mathcal{F}$ satisfies one of the following conditions: (i) P^r has treewidth $< k$; or (ii) P^r does not map homomorphically to Q^r.*

As an example, $\{K_3, \ldots, K_\ell\}$-WL is more expressive than $\{K_3, \ldots, K_{\ell-1}\}$-WL for any $\ell > 3$ because of the first condition. Similarly, $\{K_3, \ldots, K_\ell, C_m\}$-WL is more expressive than $\{K_3, \ldots, K_\ell\}$-WL for odd cycles C_m. Indeed, such cycles are cores and no clique K_ℓ with $\ell > 2$ maps homomorphically to C_m.

6 Experiments

We next showcase that GNN architectures benefit when homomorphism counts of patterns are added as additional vertex features. For patterns where homomorphism and subgraph isomorphism counts differ (e.g., cycles) we compare with GSNs [Bouritsas et al., 2020]. We use the benchmark for GNNs by Dwivedi et al. [2020], as it offers a broad choice of models, datasets and graph classification tasks.

Selected GNNs. We select the best architectures from Dwivedi et al. [2020]: Graph Attention Networks (GAT) [Velickovic et al., 2018], Graph Convolutional Networks (GCN) [Kipf and Welling, 2017], GraphSage [Hamilton et al., 2017], Gaussian Mixture Models (MoNet) [Monti et al., 2017] and GatedGCN [Bresson and Laurent, 2017]. We leave out various linear architectures such as GIN [Xu et al., 2019] as they were shown to perform poorly on the benchmark.

Learning tasks and datasets. As in Dwivedi et al. [2020] we consider (i) graph regression and the ZINC dataset [Irwin et al., 2012, Dwivedi et al., 2020]; (ii) vertex classification and the PATTERN and CLUSTER datasets [Dwivedi et al., 2020]; and (iii) link prediction and the COLLAB dataset [Hu et al., 2020]. We omit graph classification: for this task, the graph datasets from Dwivedi et al. [2020] originate from image data and hence vertex neighborhoods carry little information.

Table 1: Results for the ZINC dataset.

(a) Results for the ZINC dataset show that homomorphism (hom) counts of cycles improve every model. We compare the mean absolute error (MAE) of each model without any homomorphism count (baseline), against the model augmented with the hom count, and with subgraph isomorphism (iso) counts of C_3–C_{10}.

Model	MAE (base)	MAE (hom)	MAE (iso)
GAT	0.47±0.02	**0.22±0.01**	0.24±0.01
GCN	0.35±0.01	**0.20±0.01**	0.22±0.01
GraphSage	0.44±0.01	**0.24±0.01**	0.24±0.01
MoNet	0.25±0.01	0.19±0.01	**0.16±0.01**
GatedGCN	0.34±0.05	**0.1353±0.01**	0.1357±0.01

(b) The effect of different cycles for the GAT model over the ZINC dataset, using mean absolute error.

Set ($\mathcal{F}$)	MAE
None	0.47±0.02
$\{C_3\}$	0.45±0.01
$\{C_4\}$	0.34±0.02
$\{C_6\}$	0.31±0.01
$\{C_5, C_6\}$	0.28±0.01
$\{C_3, \ldots, C_6\}$	0.23±0.01
$\{C_3, \ldots, C_{10}\}$	**0.22±0.01**

Patterns. We extend the initial features of vertices with homomorphism counts of cycles C_ℓ of length $\ell \leq 10$, when molecular data (ZINC) is concerned, and with homomorphism counts of k-cliques K_k for $k \leq 5$, when social or collaboration data (PATTERN, CLUSTER, COLLAB) is concerned. We use the z-score of the logarithms of homomorphism counts to make them standard-normally distributed and comparable to other features. Section 5 tells us that all these patterns will increase expressive power (Theorem 4 and Proposition 5) and are "minimal" in the sense that they are not the join of smaller patterns (Proposition 6). Similar pattern choices were used in Bouritsas et al. [2020]. We use DISC [Zhang et al., 2020][3], a tool specifically built to get homomorphism counts for large graph datasets. Each model is trained and tested independently using combinations of patterns.

Higher-order GNNs. We do not compare to higher-order GNNs since this was already done by Dwivedi et al. [2020]. They included ring-GNNs (which outperform 2WL-GNNs) and 3WL-GNNs in their experiments, and these were outperformed by our selected "linear" architectures. Although the increased expressive power of higher-order GNNs may be beneficial for learning, scalability and learning issues (e.g., loss divergence) hamper their applicability [Dwivedi et al., 2020]. Our approach thus certainly outperforms higher-order GNNs with respect to the benchmark.

Methodology. Graphs were divided between training/test as instructed by Dwivedi et al. [2020], and all numbers reported correspond to the test set. The reported performance is the average over four runs with different random seeds for the respective combinations of patterns in $\mathcal{F}$, model and dataset. Training times were comparable to the baseline of training models without any augmented features.[4] All models for ZINC, PATTERN and COLLAB were trained on a GeForce GTX 1080 Ti GPU, for CLUSTER a Tesla V100-SXM3-32GB GPU was used.

Next we summarize our results for each learning task separately. Here we report results using 16 message-passing layers for ZINC, PATTERN, and CLUSTER, and 3 message-passing layers for COLLAB, as in Dwivedi et al. [2020]. In the supplementary material we report comparable results using only 4 layers for ZINC and PATTERN.

Graph regression. The first task of the benchmark is the prediction of the solubility of molecules in the ZINC dataset [Irwin et al., 2012, Dwivedi et al., 2020], a dataset of about 12 000 graphs of small size, each of them consisting of one particular molecule. The results in Table 1a show that each of our models indeed improves by adding homomorphism counts of cycles and the best result is obtained by considering all cycles. GSNs were applied to the ZINC dataset as well [Bouritsas et al., 2020]. In Table 1a we also report results by using subgraph isomorphism counts (as in GSNs): using homomorphism counts provides comparable results with using subgraph isomorphism counts although homomorphism counts are typically more efficient to compute. By looking at the full results, we see that some cycles are much more important than others. Table 1b shows which cycles have the greatest impact for the worst-performing baseline, GAT. Remarkably, adding homomorphism counts makes the GAT model competitive with the best performers of the benchmark.

[3]We thank the authors for providing us with an executable.

[4]Code to reproduce our experiments is available at https://github.com/MrRyschkov/LGP-GNN

Table 2: Results for the PATTERN dataset show that homomorphism counts improve all models except GatedGCN. We compare weighted accuracy of each model without any homomorphism count (baseline) against the model augmented with the counts of the set $\mathcal{F}$ that showed best performance (best $\mathcal{F}$).

Model + best $\mathcal{F}$	Accuracy baseline	Accuracy best
GAT $\{K_3, K_4, K_5\}$	78.83 ± 0.60	85.50 ± 0.23
GCN $\{K_3, K_4, K_5\}$	$71.42 \pm 1{,}38$	82.49 ± 0.48
GraphSage $\{K_3, K_4, K_5\}$	$70.78 \pm 0{,}19$	$85{,}85 \pm 0.15$
MoNet $\{K_3, K_4, K_5\}$	$85.90 \pm 0{,}03$	$\mathbf{86.63 \pm 0.03}$
GatedGCN $\{\emptyset\}$	86.15 ± 0.08	86.15 ± 0.08

Table 3: All models improve the Hits@50 metric over the COLLAB dataset. We compare each model without any homomorphism count (baseline) against the model augmented with the counts of the set of patterns that showed best performance (best $\mathcal{F}$).

Model + best $\mathcal{F}$	Hits@50 baseline	Hits@50 best
GAT $\{K_3\}$	50.32±0.55	52.87±0.87
GCN $\{K_3, K_4, K_5\}$	51.35±1.30	**54.60±1.01**
GraphSage $\{K_5\}$	50.33±0.68	51.39±1.23
MoNet $\{K_4\}$	49.81±1.56	51.76±1.38
GatedGCN $\{K_3\}$	51.00±2.54	51.57±0.68

Vertex classification. The next task in the benchmark corresponds to vertex classification. Here we analyze two datasets, PATTERN and CLUSTER [Dwivedi et al., 2020], both containing over 12 000 artificially generated graphs resembling social networks or communities. The task is to predict whether a vertex belongs to a particular cluster or pattern, and all results are measured using the accuracy of the classifier. Also here, our results show that homomorphism counts, this time of cliques, tend to improve the accuracy of our models. Indeed, for the PATTERN dataset we see an improvement in all models but GatedGCN (Table 2), and three models are improved in the CLUSTER dataset (reported in the supplementary material). Once again, the best performer in this task is a model that uses our extended features. Note that we do not need to compare against subgraph isomorphism counts (GSNs), because for cliques, homomorphism counts coincide with subgraph isomorphism counts (up to a constant factor).

Link prediction In our final task we consider a single graph, COLLAB [Hu et al., 2020], with over 235 000 vertices, containing information about the collaborators in an academic network, and the task at hand is to predict future collaboration. The metric used in the benchmark is the Hits@50 evaluator [Hu et al., 2020]. Here, positive collaborations are ranked among randomly sampled negative collaborations, and the metric is the ratio of positive edges that are ranked at place 50 or above. Once again, homomorphism counts of cliques improve the performance of all models, see Table 3. An interesting observation is that the best set of features (cliques) does depend on the model, although the best model uses all cliques again. We do not compare against subgraph isomorphism counts (GSNs) for the same reason as mentioned above.

Remarks. The best performers in each task use homomorphism counts, in accordance with our theoretical results, showing that such counts do extend the power of MPNNs. Homomorphism counts are also cheap to compute. For COLLAB, the largest graph in our experiments, the homomorphism counts of all patterns we used, for all vertices, could be computed by DISC [Zhang et al., 2020] in less than 3 minutes. One important remark is that *selecting* the best set of features is still a challenging endeavor. Our theoretical results help us streamline this search, but for now it is still an exploratory task. In our experiments we first looked at adding each pattern individually, and then tried with combinations of those that showed the best improvements. This feature selection strategy incurs considerable cost and needs further investigation.

7 Conclusion

We propose $\mathcal{F}$-MPNNs as an efficient way to increase the expressive power of MPNNs and showed that enriching features with homomorphism counts of small patterns is a promising add-on to any GNN architecture. Graph parameter selection and a complete characterization of when adding a new pattern to $\mathcal{F}$ adds expressive power to the $\mathcal{F}$-WL-test deserves further study.

Acknowledgments and Disclosure of Funding

The computational resources and services used in this work were provided by the HPC core facility CalcUA of the University of Antwerp, VSC (Flemish Supercomputer Center) and Imec IDLAB, funded by the Research Foundation - Flanders (FWO) and the Flemish Government. This work is also partially funded by ANID –Millennium Science Initiative Program – Code ICN17_002, Chile.

References

Emmanuel Abbe. Community detection and stochastic block models: Recent developments. *Journal of Machine Learning Research*, 18(177):1–86, 2018. URL http://jmlr.org/papers/v18/16-480.html.

Ralph Abboud, İsmail İlkan Ceylan, Martin Grohe, and Thomas Lukasiewicz. The surprising power of graph neural networks with random node initialization. In *Proceedings of the 30th International Joint Conference on Artificial Intelligence*, pages 2112–2118, 2021. URL https://doi.org/10.24963/ijcai.2021/291.

Vikraman Arvind, Frank Fuhlbrück, Johannes Köbler, and Oleg Verbitsky. On Weisfeiler-Leman invariance: Subgraph counts and related graph properties. *Journal of Computer and System Sciences*, 113:42 – 59, 2020. URL https://doi.org/10.1016/j.jcss.2020.04.003.

Albert Atserias, Andrei A. Bulatov, and Víctor Dalmau. On the power of k-consistency. In *Proceedings of the 34th International Colloquium on Automata, Languages and Programming*, volume 4596 of *Lecture Notes in Computer Science*, pages 279–290, 2007. URL https://doi.org/10.1007/978-3-540-73420-8_26.

Waiss Azizian and Marc Lelarge. Expressive power of invariant and equivariant graph neural networks. In *International Conference on Learning Representations*, 2021. URL https://openreview.net/forum?id=lxHgXYN4bwl.

Mikhail Belkin and Partha Niyogi. Laplacian eigenmaps for dimensionality reduction and data representation. *Neural Computation*, 15(6):1373–1396, 2003. URL https://ieeexplore.ieee.org/document/6789755.

Hans L. Bodlaender. A linear time algorithm for finding tree-decompositions of small treewidth. In *Proceedings of the 25th Annual ACM Symposium on Theory of Computing*, page 226–234, 1993. URL https://doi.org/10.1145/167088.167161.

Giorgos Bouritsas, Fabrizio Frasca, Stefanos Zafeiriou, and Michael M. Bronstein. Improving graph neural network expressivity via subgraph isomorphism counting. In *Graph Representation Learning and Beyond (GRL+) Workshop at the 37th International Conference on Machine Learning*, 2020. URL https://arxiv.org/abs/2006.09252.

Simone Bova and Hubie Chen. How many variables are needed to express an existential positive query? *Theory Comput. Syst.*, 63(7):1573–1594, 2019. URL https://doi.org/10.1007/s00224-018-9884-z.

Xavier Bresson and Thomas Laurent. Residual gated graph convnets. *arXiv*, 2017. URL https://arxiv.org/abs/1711.07553.

Jin-Yi Cai, Martin Fürer, and Neil Immerman. An optimal lower bound on the number of variables for graph identifications. *Combinatorica*, 12(4):389–410, 1992. URL https://doi.org/10.1007/BF01305232.

Ines Chami, Sami Abu-El-Haija, Bryan Perozzi, Christopher Ré, and Kevin Murphy. Machine learning on graphs: A model and comprehensive taxonomy. *arXiv*, 2021. URL https://arxiv.org/abs/2005.03675.

Ting Chen, Song Bian, and Yizhou Sun. Are powerful graph neural nets necessary? A dissection on graph classification. *arXiv*, 2019a. URL https://arxiv.org/abs/1905.04579.

Zhengdao Chen, Soledad Villar, Lei Chen, and Joan Bruna. On the equivalence between graph isomorphism testing and function approximation with GNNs. In *Advances in Neural Information Processing Systems*, volume 32, pages 15894–15902, 2019b. URL https://proceedings.neurips.cc/paper/2019/file/71ee911dd06428a96c143a0b135041a4-Paper.pdf.

Zhengdao Chen, Lei Chen, Soledad Villar, and Joan Bruna. Can graph neural networks count substructures? In *Advances in Neural Information Processing Systems*, volume 33, 2020. URL https://proceedings.neurips.cc/paper/2020/file/75877cb75154206c4e65e76b88a12712-Paper.pdf.

Radu Curticapean, Holger Dell, and Dániel Marx. Homomorphisms are a good basis for counting small subgraphs. In *Proceedings of the 49th Symposium on Theory of Computing*, pages 210—223, 2017. URL http://dx.doi.org/10.1145/3055399.3055502.

Holger Dell, Martin Grohe, and Gaurav Rattan. Lovász meets Weisfeiler and Leman. In *Proceedings of the 45th International Colloquium on Automata, Languages, and Programming*, volume 107, pages 40:1–40:14, 2018. URL https://doi.org/10.4230/LIPIcs.ICALP.2018.40.

Zdenek Dvorak. On recognizing graphs by numbers of homomorphisms. *Journal of Graph Theory*, 64(4):330–342, 2010. URL https://doi.org/10.1002/jgt.20461.

Vijay Prakash Dwivedi, Chaitanya K Joshi, Thomas Laurent, Yoshua Bengio, and Xavier Bresson. Benchmarking graph neural networks. *arXiv*, 2020. URL https://arxiv.org/abs/2003.00982.

Josep Díaz, Maria Serna, and Dimitrios M. Thilikos. Counting H-colorings of partial k-trees. *Theoretical Computer Science*, 281(1):291–309, 2002. URL https://doi.org/10.1016/S0304-3975(02)00017-8.

Vikas K. Garg, Stefanie Jegelka, and Tommi S. Jaakkola. Generalization and representational limits of graph neural networks. In *Proceedings of the 37th International Conference on Machine Learning*, volume 119, pages 3419–3430, 2020. URL http://proceedings.mlr.press/v119/garg20c.html.

Floris Geerts. The expressive power of kth-order invariant graph networks. *arXiv*, 2020. URL https://arxiv.org/abs/2007.12035.

Floris Geerts, Filip Mazowiecki, and Guillermo A. Pérez. Let's agree to degree: Comparing graph convolutional networks in the message-passing framework. In *Proceedings of the 38th International Conference on Machine Learning*, 2021. URL https://arxiv.org/abs/2004.02593.

Justin Gilmer, Samuel S. Schoenholz, Patrick F. Riley, Oriol Vinyals, and George E. Dahl. Neural message passing for quantum chemistry. In *Proceedings of the 34th International Conference on Machine Learning*, volume 70, pages 1263–1272, 2017. URL http://proceedings.mlr.press/v70/gilmer17a/gilmer17a.pdf.

Martin Grohe. *Descriptive Complexity, Canonisation, and Definable Graph Structure Theory*. Lecture Notes in Logic. Cambridge University Press, 2017. URL https://doi.org/10.1017/9781139028868.

Martin Grohe. word2vec, node2vec, graph2vec, x2vec: Towards a theory of vector embeddings of structured data. In *Proceedings of the 39th Symposium on Principles of Database Systems*, pages 1–16, 2020a. URL https://doi.org/10.1145/3375395.3387641.

Martin Grohe. Counting bounded tree depth homomorphisms. In *Proceedings of the 35th Symposium on Logic in Computer Science*, pages 507–520, 2020b. URL https://doi.org/10.1145/3373718.3394739.

William L. Hamilton, Zhitao Ying, and Jure Leskovec. Inductive representation learning on large graphs. In *Advances in Neural Information Processing Systems*, volume 30, pages 1024–1034, 2017.

Lauri Hella. Logical hierarchies in PTIME. *Inf. Comput.*, 129(1):1–19, 1996. URL https://doi.org/10.1006/inco.1996.0070.

Weihua Hu, Matthias Fey, Marinka Zitnik, Yuxiao Dong, Hongyu Ren, Bowen Liu, Michele Catasta, and Jure Leskovec. Open graph benchmark: Datasets for machine learning on graphs. In *Advances in Neural Information Processing Systems*, volume 33, 2020. URL https://arxiv.org/abs/2005.00687.

John J. Irwin, Teague Sterling, Michael M. Mysinger, Erin S. Bolstad, and Ryan G. Coleman. Zinc: A free tool to discover chemistry for biology. *Journal of Chemical Information and Modeling*, 52 (7):1757–1768, 2012. URL https://doi.org/10.1021/ci3001277.

Katsuhiko Ishiguro, Kenta Oono, and Kohei Hayashi. Weisfeiler-Lehman embedding for molecular graph neural networks. *arXiv*, 2020. URL https://arxiv.org/abs/2006.06909.

Nicolas Keriven and Gabriel Peyré. Universal invariant and equivariant graph neural networks. In *Advances in Neural Information Processing Systems*, volume 32, pages 7092–7101, 2019. URL https://proceedings.neurips.cc/paper/2019/file/ea9268cb43f55d1d12380fb6ea5bf572-Paper.pdf.

Thomas N. Kipf and Max Welling. Semi-supervised classification with graph convolutional networks. In *International Conference on Learning Representations*, 2017. URL https://openreview.net/forum?id=SJU4ayYgl.

Alexandre Lacoste, Alexandra Luccioni, Victor Schmidt, and Thomas Dandres. Quantifying the carbon emissions of machine learning. *arXiv preprint arXiv:1910.09700*, 2019.

Michael Lingzhi Li, Meng Dong, Jiawei Zhou, and Alexander M. Rush. A hierarchy of graph neural networks based on learnable local features. *arXiv*, 2019. URL https://arxiv.org/abs/1911.05256.

Andreas Loukas. What graph neural networks cannot learn: depth vs width. In *International Conference on Learning Representations*, 2020. URL https://openreview.net/forum?id=B1l2bp4YwS.

Haggai Maron, Heli Ben-Hamu, Hadar Serviansky, and Yaron Lipman. Provably powerful graph networks. In *Advances in Neural Information Processing Systems*, volume 32, pages 2153–2164, 2019a. URL http://papers.nips.cc/paper/8488-provably-powerful-graph-networks.

Haggai Maron, Ethan Fetaya, Nimrod Segol, and Yaron Lipman. On the universality of invariant networks. In *Proceedings of the 36th International Conference on Machine Learning*, volume 97, pages 4363–4371, 2019b. URL http://proceedings.mlr.press/v97/maron19a.html.

Christian Merkwirth and Thomas Lengauer. Automatic generation of complementary descriptors with molecular graph networks. *J. Chem. Inf. Model.*, 45(5):1159–1168, 2005. URL https://pubs.acs.org/doi/pdf/10.1021/ci049613b.

Federico Monti, Davide Boscaini, Jonathan Masci, Emanuele Rodola, Jan Svoboda, and Michael M Bronstein. Geometric deep learning on graphs and manifolds using mixture model CNNs. In *Proceedings of the IEEE conference on computer vision and pattern recognition*, pages 5115–5124, 2017. URL https://openaccess.thecvf.com/content_cvpr_2017/papers/Monti_Geometric_Deep_Learning_CVPR_2017_paper.pdf.

Christopher Morris, Martin Ritzert, Matthias Fey, William L. Hamilton, Jan Eric Lenssen, Gaurav Rattan, and Martin Grohe. Weisfeiler and Leman go neural: Higher-order graph neural networks. In *Proceedings of the 33rd AAAI Conference on Artificial Intelligence*, pages 4602–4609, 2019. URL https://doi.org/10.1609/aaai.v33i01.33014602.

Christopher Morris, Gaurav Rattan, and Petra Mutzel. Weisfeiler and leman go sparse: Towards scalable higher-order graph embeddings. In *Advances in Neural Information Processing Systems*, volume 33, 2020. URL https://arxiv.org/abs/1904.01543.

Hoang NT and Takanori Maehara. Graph homomorphism convolution. In *Proceedings of the 37th International Conference on Machine Learning*, pages 7306–7316, 2020. URL http://proceedings.mlr.press/v119/nguyen20c.html.

Martin Otto. *Bounded Variable Logics and Counting: A Study in Finite Models*, volume 9 of *Lecture Notes in Logic*. Cambridge University Press, 2017. URL https://doi.org/10.1017/9781316716878.

Ryoma Sato. A survey on the expressive power of graph neural networks. *arXiv*, 2020. URL https://arxiv.org/abs/2003.04078.

Ryoma Sato, Makoto Yamada, and Hisashi Kashima. Approximation ratios of graph neural networks for combinatorial problems. In *Advances in Neural Information Processing Systems*, volume 32, pages 4083–4092, 2019. URL https://papers.nips.cc/paper/2019/file/635440afdfc39fe37995fed127d7df4f-Paper.pdf.

Ryoma Sato, Makoto Yamada, and Hisashi Kashima. Random features strengthen graph neural networks. In *Proceedings of the 2021 SIAM International Conference on Data Mining*, pages 333–341, 2021. URL https://doi.org/10.1137/1.9781611976700.38.

Franco Scarselli, Marco Gori, Ah Chung Tsoi, Markus Hagenbuchner, and Gabriele Monfardini. The graph neural network model. *IEEE Trans. Neural Networks*, 20(1):61–80, 2009. URL https://doi.org/10.1109/TNN.2008.2005605.

Nino Shervashidze, S.V.N. Vishwanathan, Tobias Petri, Kurt Mehlhorn, and Karsten Borgwardt. Efficient graphlet kernels for large graph comparison. In *Proceedings of the 12th International Conference on Artificial Intelligence and Statistics*, volume 5, pages 488–495, 2009. URL http://proceedings.mlr.press/v5/shervashidze09a.html.

Behrooz Tahmasebi and Stefanie Jegelka. Counting substructures with higher-order graph neural networks: Possibility and impossibility results. *arXiv*, 2020. URL https://arxiv.org/abs/2012.03174.

Petar Velickovic, Guillem Cucurull, Arantxa Casanova, Adriana Romero, Pietro Liò, and Yoshua Bengio. Graph attention networks. In *International Conference on Learning Representations*, 2018. URL https://openreview.net/forum?id=rJXMpikCZ.

Clément Vignac, Andreas Loukas, and Pascal Frossard. Building powerful and equivariant graph neural networks with structural message-passing. In *Advances in Neural Information Processing Systems*, volume 33, 2020. URL https://proceedings.neurips.cc/paper/2020/hash/a32d7eeaae19821fd9ce317f3ce952a7-Abstract.html.

Boris J. Weisfeiler and Andrei A. Lehman. A reduction of a graph to a canonical form and an algebra arising during this reduction. *Nauchno-Technicheskaya Informatsiya*, 2(9):12–16, 1968. https://www.iti.zcu.cz/wl2018/pdf/wl_paper_translation.pdf.

Z. Wu, S. Pan, F. Chen, G. Long, C. Zhang, and P. S. Yu. A comprehensive survey on graph neural networks. *IEEE Transactions on Neural Networks and Learning Systems*, 32(1):4–24, 2021. URL https://doi.org/10.1109/TNNLS.2020.2978386.

Keyulu Xu, Weihua Hu, Jure Leskovec, and Stefanie Jegelka. How powerful are graph neural networks? In *International Conference on Learning Representations*, 2019. URL https://openreview.net/forum?id=ryGs6iA5Km.

Hao Zhang, Jeffrey Xu Yu, Yikai Zhang, Kangfei Zhao, and Hong Cheng. Distributed subgraph counting: A general approach. *Proc. VLDB Endow.*, 13(11):2493–2507, 2020. URL http://www.vldb.org/pvldb/vol13/p2493-zhang.pdf.

Jie Zhou, Ganqu Cui, Zhengyan Zhang, Cheng Yang, Zhiyuan Liu, and Maosong Sun. Graph neural networks: A review of methods and applications. *ArXiv*, 2018. URL http://arxiv.org/abs/1812.08434.

A Proofs of Section 3

We use the following notions. Let G and H be graphs, $v \in V_G$, $w \in V_H$, and $d \geq 0$. The vertices v and w are said to be indistinguishably by $\mathcal{F}$-WL in round d, denoted by $(G,v) \equiv^{(d)}_{\mathcal{F}\text{-WL}} (H,w)$, iff $\chi^{(d)}_{\mathcal{F},G,v} = \chi^{(d)}_{\mathcal{F},H,w}$. Similarly, G and H are said to be indistinguishable by $\mathcal{F}$-WL in round d, denoted by $G \equiv^{(d)}_{\mathcal{F}\text{-WL}} H$, iff $\{\!\{\chi^{(d)}_{\mathcal{F},G,v} \mid v \in V_G\}\!\} = \{\!\{\chi^{(d)}_{\mathcal{F},H,w} \mid w \in V_H\}\!\}$. Along the same lines, v and w are indistinguishable by an $\mathcal{F}$-MPNN M, denoted by $(G,v) \equiv^{(d)}_{M,\mathcal{F}} (H,w)$, iff $\mathbf{x}^{(d)}_{M,\mathcal{F},G,v} = \mathbf{x}^{(d)}_{M,\mathcal{F},H,w}$. Similarly, G and H are said to be indistinguishable by M in round d, denoted by $G \equiv^{(d)}_{M,\mathcal{F}} H$, iff $\{\!\{\mathbf{x}^{(d)}_{M,\mathcal{F},G,v} \mid v \in V_G\}\!\} = \{\!\{\mathbf{x}^{(d)}_{M,\mathcal{F},H,w} \mid w \in V_H\}\!\}$.

A.1 Proof of Proposition 1

We show that the class of $\mathcal{F}$-MPNNs is upper bounded in expressive power by $\mathcal{F}$-WL. The proof is analogous to the proof in Morris et al. [2019] showing that MPNNs are bounded by WL.

We show a stronger result by upper bounding $\mathcal{F}$-MPNNs by $\mathcal{F}$-WL-test, layer by layer. More precisely, we show that for every $\mathcal{F}$-MPNN M, graphs G and H, vertices $v \in V_G$, $w \in V_H$, and $d \geq 0$,

(1) $(G,v) \equiv^{(d)}_{\mathcal{F}\text{-WL}} (H,w) \implies (G,v) \equiv^{(d)}_{M,\mathcal{F}} (H,w)$; and
(2) $G \equiv^{(d)}_{\mathcal{F}\text{-WL}} H \implies G \equiv^{(d)}_{M,\mathcal{F}} H$.

Clearly, these imply that $\mathcal{F}$-MPNNs are bounded in expressive power by $\mathcal{F}$-WL, both when vertex and graph distinguishability are concerned.

Proof of implication (1). We show this implication by induction on the number of rounds.

Base case. We first assume $(G,v) \equiv^{(0)}_{\mathcal{F}\text{-WL}} (H,w)$. In other words, $\chi^{(0)}_{\mathcal{F},G,v} = \chi^{(0)}_{\mathcal{F},H,w}$ and thus, $\chi_G(v) = \chi_H(w)$ and for every $P^r \in \mathcal{F}$ we have $\mathsf{hom}(P^r, G^v) = \mathsf{hom}(P^r, H^w)$. By definition, $\mathbf{x}^{(0)}_{M,\mathcal{F},G,v}$ is a hot-one encoding of $\chi_G(v)$ combined with $\mathsf{hom}(P^r, G^v)$ for $P^r \in \mathcal{F}$, for every MPNN M, graph G and vertex $v \in V_G$. Since these agree with the labelling and homomorphism counts for vertex $w \in V_H$ in graph H, we also have that $\mathbf{x}^{(0)}_{M,\mathcal{F},G,v} = \mathbf{x}^{(0)}_{M,\mathcal{F},H,w}$, as desired.

Inductive step. We next assume $(G,v) \equiv^{(d)}_{\mathcal{F}\text{-WL}} (H,w)$. By the definition of $\mathcal{F}$-WL this is equivalent to $(G,v) \equiv^{(d-1)}_{\mathcal{F}\text{-WL}} (H,w)$ and $\{\!\{\chi^{(d-1)}_{\mathcal{F},G,v'} \mid v' \in N_G(v)\}\!\} = \{\!\{\chi^{(d-1)}_{\mathcal{F},H,w'} \mid w' \in N_H(w)\}\!\}$. By the induction hypothesis, this implies $(G,v) \equiv^{(d-1)}_{M,\mathcal{F}} (H,w)$ and there exists a bijection $\beta : N_G(v) \to N_H(w)$ such that $(G,v') \equiv^{(d-1)}_{M,\mathcal{F}} (H,\beta(v'))$ for every $v' \in N_G(v)$, and every $\mathcal{F}$-MPNN M. In other words, $\mathbf{x}^{(d-1)}_{M,\mathcal{F},G,v} = \mathbf{x}^{(d-1)}_{M,\mathcal{F},H,w}$ and $\mathbf{x}^{(d-1)}_{M,\mathcal{F},G,v'} = \mathbf{x}^{(d-1)}_{M,\mathcal{F},H,\beta(v')}$ for every $v' \in N_G(v)$. By the definition of $\mathcal{F}$-MPNNs this implies that $\textsc{Comb}^{(d)}\big(\{\!\{\mathbf{x}^{(d-1)}_{M,\mathcal{F},G,v'} \mid v' \in N_G(v)\}\!\}\big)$ is equal to $\textsc{Comb}^{(d)}\big(\{\!\{\mathbf{x}^{(d-1)}_{M,\mathcal{F},H,w'} \mid w' \in N_H(w)\}\!\}\big)$ and hence also, after applying $\textsc{Upd}^{(d)}$, $\mathbf{x}^{(d)}_{M,\mathcal{F},G,v} = \mathbf{x}^{(d)}_{M,\mathcal{F},H,w}$. That is, $(G,u) \equiv^{(d)}_{M,\mathcal{F}} (H,w)$, as desired.

Proof of implication (2). The implication $G \equiv^{(d)}_{\mathcal{F}\text{-WL}} H \implies G \equiv^{(d)}_{M,\mathcal{F}} H$ now easily follows. Indeed, $G \equiv^{(d)}_{\mathcal{F}\text{-WL}} H$ is equivalent to $\{\!\{\chi^{(d)}_{\mathcal{F},G,v} \mid v \in V_G\}\!\} = \{\!\{\chi^{(d)}_{\mathcal{F},H,w} \mid w \in V_H\}\!\}$. In other words, there exists a bijection $\alpha : V_G \to V_H$ such that $\chi^{(d)}_{\mathcal{F},G,v} = \chi^{(d)}_{\mathcal{F},H,\alpha(v)}$ for every $v \in V_G$. We have just shown that this implies $\mathbf{x}^{(d)}_{M,\mathcal{F},G,v} = \mathbf{x}^{(d)}_{M,\mathcal{F},H,\alpha(v)}$ for every $v \in V_G$ and for every $\mathcal{F}$-MPNN M. Hence, $\{\!\{\mathbf{x}^{(d)}_{M,\mathcal{F},G,v} \mid v \in V_G\}\!\} = \{\!\{\mathbf{x}^{(d)}_{M,\mathcal{F},H,w} \mid w \in V_H\}\!\}$, or $G \equiv^{(d)}_{M,\mathcal{F}} H$, as desired. □

A.2 Proof of Theorem 1

We show that for any finite collection $\mathcal{F}$ of patterns, graphs G and H, vertices $v \in V_G$ and $w \in V_H$, and $d \geq 0$:

$$(G, v) \equiv^{(d)}_{\mathcal{F}\text{-WL}} (H, w) \iff \mathsf{hom}(T^r, G^v) = \mathsf{hom}(T^r, H^w), \tag{1}$$

for every $\mathcal{F}$-pattern tree T^r of depth at most d. Similarly,

$$G \equiv^{(d)}_{\mathcal{F}\text{-WL}} H \iff \mathsf{hom}(T, G) = \mathsf{hom}(T, H), \tag{2}$$

for every (unrooted) $\mathcal{F}$-pattern tree of depth at most d.

For a given set $\mathcal{F} = \{P_1^r, \ldots, P_\ell^r\}$ of patterns and $\mathbf{s} = (s_1, \ldots, s_\ell) \in \mathbb{N}^\ell$, we denote by $\mathcal{F}^{\mathbf{s}}$ the graph pattern of the form $(P_1^{s_1} \star \cdots \star P_\ell^{s_\ell})^r$, that is, we join s_1 copies of P_1, s_2 copies of P_2 and so on.

Proof of equivalence (1). The proof is by induction on the number of rounds d.

$\boxed{\Longrightarrow}$ We first consider the implication $(G, v) \equiv^{(d)}_{\mathcal{F}\text{-WL}} (H, w) \Longrightarrow \mathsf{hom}(T^r, G^v) = \mathsf{hom}(T^r, H^w)$ for every $\mathcal{F}$-pattern tree T^r of depth at most d.

Base case. Let us first consider the base case, that is, $d = 0$. In other words, we consider $\mathcal{F}$-pattern trees T^r consisting of a single root r adorned with a pattern $\mathcal{F}^{\mathbf{s}}$ for some $\mathbf{s} = (s_1, \ldots, s_\ell) \in \mathbb{N}^\ell$. We note that due to the properties of the graph join operator:

$$\mathsf{hom}(T^r, G^v) = \prod_{i=1}^{\ell} \big(\mathsf{hom}(P_i^r, G^v)\big)^{s_i}. \tag{3}$$

Since, $(G, v) \equiv^{(0)}_{\mathcal{F}\text{-WL}} (H, w)$, we know that $\chi_G(v) = \chi_H(w) = a$ for some $a \in \Sigma$ and $\mathsf{hom}(P_i^r, G^v) = \mathsf{hom}(P_i^r, H^w)$ for all $P_i^r \in \mathcal{F}$. This implies that the product in (3) is equal to

$$\prod_{i=1}^{\ell} \big(\mathsf{hom}(P_i^r, H^w)\big)^{s_i} = \mathsf{hom}(T^r, H^w),$$

as desired.

Inductive step. Suppose next that we know that the implication holds for $d-1$. We assume now $(G, v) \equiv^{(d)}_{\mathcal{F}\text{-WL}} (H, w)$ and consider an $\mathcal{F}$-pattern tree T^r of depth at most d. Assume that in the backbone of T^r, the root r has m children $c_1, \ldots, c_m$, and denote by $T_1^{c_1}, \ldots, T_m^{c_\ell}$ the $\mathcal{F}$-pattern trees in T^r rooted at c_i. Furthermore, we denote by $T_i^{(r,c_i)}$ the $\mathcal{F}$-pattern tree obtained from $T_i^{c_i}$ by attaching r to c_i; $T_i^{(r,c_i)}$ has root r. Let $\mathcal{F}^{\mathbf{s}}$ be the pattern in T^r associated with r. The following equalities are readily verified:

$$\mathsf{hom}(T^r, G^v) = \mathsf{hom}(\mathcal{F}^{\mathbf{s}}, G^v) \prod_{i=1}^{m} \mathsf{hom}(T_i^{(r,c_i)}, G^v) = \mathsf{hom}(\mathcal{F}^{\mathbf{s}}, G^v) \prod_{i=1}^{m} \Big(\sum_{v' \in N_G(v)} \mathsf{hom}(T_i^{c_i}, G^{v'}) \Big). \tag{4}$$

Recall now that we assume $(G, v) \equiv^{(d)}_{\mathcal{F}\text{-WL}} (H, w)$ and thus, in particular, $(G, v) \equiv^{(0)}_{\mathcal{F}\text{-WL}} (H, w)$. Hence, by induction, $\mathsf{hom}(S^r, G^v) = \mathsf{hom}(S^r, H^w)$ for every $\mathcal{F}$-pattern tree S^r of depth 0. In particular, this holds for $S^r = \mathcal{F}^{\mathbf{s}}$ and hence

$$\mathsf{hom}(\mathcal{F}^{\mathbf{s}}, G^v) = \mathsf{hom}(\mathcal{F}^{\mathbf{s}}, H^w).$$

Furthermore, $(G, v) \equiv^{(d)}_{\mathcal{F}\text{-WL}} (H, w)$ implies that there exists a bijection $\beta : N_G(v) \to N_H(w)$ such that $(G, v') \equiv^{(d-1)}_{\mathcal{F}\text{-WL}} (H, \beta(v'))$ for every $v' \in N_G(v)$. By induction, for every $v' \in N_G(v)$ there thus exists a unique $w' \in N_H(w)$ such that $\mathsf{hom}(S^r, G^{v'}) = \mathsf{hom}(S^r, H^{w'})$ for every $\mathcal{F}$-pattern tree S^r of depth at most $d-1$. In particular, for every $v' \in N_G(v)$ there exists a $w' \in N_H(w)$ such that

$$\mathsf{hom}(T_i^{c_i}, G^{v'}) = \mathsf{hom}(T_i^{c_i}, H^{w'}),$$

for each of the sub-trees $T_i^{c_i}$ in T^r. Hence, (4) is equal to

$$\mathsf{hom}(\mathcal{F}^{\mathbf{s}}, H^w)\prod_{i=1}^{m}\Big(\sum_{w'\in N_H(w)}\mathsf{hom}(T_i^{c_i}, H^{w'})\Big),$$

which in turn is equal to $\mathsf{hom}(T^r, H^w)$, as desired.

$\boxed{\Longleftarrow}$ We next consider the other direction, that is, we show that when $\mathsf{hom}(T^r, G^v) = \mathsf{hom}(S^r, H^w)$ holds for every $\mathcal{F}$-pattern tree T^r of depth at most d, then $(G, v) \equiv^{(d)}_{\mathcal{F}\text{-WL}} (H, w)$ holds. This is again verified by induction on d. This direction is more complicated and is similar to techniques used in Grohe [2020b]. In our induction hypothesis we further include that a *finite* number of $\mathcal{F}$-pattern trees suffices to infer $(G, v) \equiv^{(d)}_{\mathcal{F}\text{-WL}} (H, w)$ for graphs G and H and vertices $v \in V_G$ and $w \in V_H$.

Base case. Let us consider the base case $d = 0$ first. We need to show that $\chi_G(v) = \chi_H(w)$ and $\mathsf{hom}(P_i^r, G^v) = \mathsf{hom}(P_i^r, H^w)$ for every $P_i^r \in \mathcal{F}$, since this implies $(G, v) \equiv^{(0)}_{\mathcal{F}\text{-WL}} (H, w)$.

We first observe that $\mathsf{hom}(T^r, G^v) = \mathsf{hom}(T^r, H^w)$ for every $\mathcal{F}$-pattern tree T^r of depth 0, implies that v and w must be assigned the same label, say a, by χ_G and χ_H, respectively.

Indeed, if we take T^r to consist of a single root r labeled with a (and thus r is associated with the pattern $\mathcal{F}^{\mathbf{0}}$), then $\mathsf{hom}(T^r, G^v) = \mathsf{hom}(T^r, H^w)$ will be one if $\chi_G(v) = \chi_H(w) = a$ and zero otherwise. This implies that $\chi_G(v) = \chi_H(w) = a$.

Next, we show that $\mathsf{hom}(P_i^r, G^v) = \mathsf{hom}(P_i^r, H^w)$ for every $P_i^r \in \mathcal{F}$. It suffices to consider the $\mathcal{F}$-pattern tree T_i^r consisting of a root r joined with a single copy of P_i^r.

We observe that we only need a finite number of $\mathcal{F}$-pattern trees to infer $(G, v) \equiv^{(0)}_{\mathcal{F}\text{-WL}} (H, w)$. Indeed, suppose that χ_G and χ_H assign labels $a_1, \dots, a_L$, then we need L single vertex trees with no patterns attached and root labeled with one of these labels. In addition, we need one $\mathcal{F}$-pattern tree for each pattern $P_i^r \in \mathcal{F}$ and each label $a_1, \dots, a_L$. That is, we need $L(\ell + 1)$ $\mathcal{F}$-pattern trees of depth 0.

Inductive step. We now assume that the implication holds for $d - 1$ and consider d. That is, we assume that if $\mathsf{hom}(T^r, G^v) = \mathsf{hom}(T^r, H^w)$ holds for every $\mathcal{F}$-pattern tree T^r of depth at most $d - 1$, then $(G, v) \equiv^{(d-1)}_{\mathcal{F}\text{-WL}} (H, w)$ holds. Furthermore, we assume that only a finite number K of $\mathcal{F}$-pattern trees $S_1^r, \dots, S_K^r$ of depth at most $d - 1$ suffice to infer $(G, v) \equiv^{(d-1)}_{\mathcal{F}\text{-WL}} (H, w)$.

So, for d, let us assume that $\mathsf{hom}(T^r, G^v) = \mathsf{hom}(T^r, H^w)$ holds for every $\mathcal{F}$-pattern tree of depth at most d. We need to show $(G, v) \equiv^{(d)}_{\mathcal{F}\text{-WL}} (H, w)$ and that we can again assume that a finite number of $\mathcal{F}$-pattern trees of depth at most d suffice to infer $(G, v) \equiv^{(d)}_{\mathcal{F}\text{-WL}} (H, w)$.

By definition of $(G, v) \equiv^{(d)}_{\mathcal{F}\text{-WL}} (H, w)$, we can, equivalently, show that $(G, v) \equiv^{(d-1)}_{\mathcal{F}\text{-WL}} (H, w)$ and that there exists a bijection $\beta : N_G(v) \to N_H(w)$ such that $(G, v') \equiv^{(d-1)}_{\mathcal{F}\text{-WL}} (H, \beta(v'))$ for every $v' \in N_G(v)$. That $(G, v) \equiv^{(d-1)}_{\mathcal{F}\text{-WL}} (H, w)$ holds, is by induction, since $\mathsf{hom}(T^r, G^v) = \mathsf{hom}(T^r, H^w)$ for every $\mathcal{F}$-pattern tree of depth at most d and thus also for every $\mathcal{F}$-pattern tree of depth at most $d - 1$. We may thus focus on showing the existence of the bijection β.

Let $X, Y \in \{G, H\}$, $x \in V_X$ and $y \in V_Y$. We know, by induction and the proof of the previous implication, that $(X, x) \equiv^{(d-1)}_{\mathcal{F}\text{-WL}} (Y, y)$ if and only if $\mathsf{hom}(S_i^r, X^x) = \mathsf{hom}(S_i^r, Y^y)$ for each $i \in K$. Denote by $R_1, \dots, R_e$ the equivalence class on $V_X \cup V_Y$ induced by $\equiv^{(d-1)}_{\mathcal{F}\text{-WL}}$. Furthermore, define $N_{j,X}(x) := N_X(x) \cap R_j$ and let $n_j = |N_{j,G}(v)|$ and $m_j = |N_{j,H}(w)|$ for $v \in V_G$ and $w \in V_H$, for each $j \in [e]$. If we can show that $n_j = m_j$ for each $j \in [e]$, then this implies the existence of the desired bijection.

Let $T_i^{r=a}$ be the $\mathcal{F}$-pattern tree of depth at most d obtained by attaching S_i^r to a new root vertex r labeled with a. We may assume that v and w both have label a, since their homomorphism counts for the single root trees with labels from Σ. The root vertex r is not joined with any $\mathcal{F}^{\mathbf{s}}$ (or alternatively it is joined with $\mathcal{F}^{\mathbf{0}}$). It will be convenient to denote the root of S_i^r by r_i instead of r. Then for each

$i \in [K]$:

$$\begin{aligned}\mathsf{hom}(T_i^{r=a}, G^v) &= \sum_{v' \in N_G(v)} \mathsf{hom}(S_i^{r_i}, G^{v'}) = \sum_{j\in[e]} n_j \mathsf{hom}(S_i^{r_i}, G^{v'_j}) \\ &= \sum_{j\in[e]} m_j \mathsf{hom}(S_i^{r_i}, H^{w'_j}) = \sum_{w'\in N_H(w)} \mathsf{hom}(S_i^{r_i}, H^{w'}) = \mathsf{hom}(T_i^{r=a}, H^w),\end{aligned}$$

where v'_j and w'_j denote arbitrary vertices in $N_{j,G}(v)$ and $N_{j,H}(w)$, respectively. Let us denote $\mathsf{hom}(S_i^{r_i}, G^{v'_j})$ by a_{ij} and observe that this is equal to $\mathsf{hom}(S_i^{r_i}, H^{w'_j})$. Hence, we know that for each $i \in [K]$:

$$\sum_{j\in[e]} a_{ij} n_j = \sum_{j\in[e]} a_{ij} m_j.$$

Let us call a set $I \subseteq [K]$ compatible if all roots in $S_i^{r_i}$, for $i \in I$, have the same label. Consider a vector $\mathbf{s} = (s_1, \dots, s_K) \in \mathbb{N}^K$ and define its support as $\mathsf{supp}(\mathbf{s}) := \{i \in [K] \mid s_i \neq 0\}$. We say that $\mathbf{s}$ is compatible if its support is. For such a compatible $\mathbf{s}$ we now define $T^{r=a,\mathbf{s}}$ to be the $\mathcal{F}$-pattern tree with root r labeled with a, with one child c which is joined with (and inheriting the label from) the following $\mathcal{F}$-pattern tree of depth $d-1$:

$$\bigstar_{i\in\mathsf{supp}(\mathbf{s})} S_i^{s_i}.$$

In other words, we simply join together powers of the $S_i^{r_i}$'s that have roots with the same label. Then for every compatible $\mathbf{s} \in \mathbb{N}^K$:

$$\begin{aligned}\mathsf{hom}(T^{r=a,\mathbf{s}}, G^v) &= \sum_{v'\in N_G(v)} \prod_{i\in[K]} \big(\mathsf{hom}(S_i^{r_i}, G^{v'})\big)^{s_i} = \sum_{j\in[e]} n_j \prod_{i\in[K]} \big(\mathsf{hom}(S_i^{r_i}, G^{v'_j})\big)^{s_i} \\ &= \sum_{j\in[e]} m_j \prod_{i\in[K]} \big(\mathsf{hom}(S_i^{r_i}, H^{w'_j})\big)^{s_i} = \sum_{w'\in N_H(w)} \prod_{i\in[K]} \big(\mathsf{hom}(S_i^{r_i}, H^{w'})\big)^{s_i} \\ &= \mathsf{hom}(T_i^{r=a,\mathbf{s}}, H^w),\end{aligned}$$

where, as before, v'_j and w'_j denote arbitrary vertices in $N_{j,G}(v)$ and $N_{j,H}(w)$, respectively. Hence, for any compatible $\mathbf{s} \in \mathbb{N}^K$:

$$\sum_{j\in[e]} n_j \prod_{i\in[K]} a_{ij}^{s_i} = \sum_{j\in[e]} m_j \prod_{i\in[K]} a_{ij}^{s_i}.$$

We now continue in the same way as in the proof of Lemma 4.2 in Grohe [2020b]. We repeat the argument here for completeness. Define $\mathbf{a}_j^{\mathbf{s}} := \prod_{i=1}^K a_{ij}^{s_i}$ for each $j \in [e]$. We assume, for the sake of contradiction, that there exists a $j \in [e]$ such that $n_j \neq m_j$. We choose such a $j_0 \in [e]$ for which $S = \mathsf{supp}(\mathbf{a}_{j_0})$ is inclusion-wise maximal.

We first rule out that $S = \emptyset$. Indeed, suppose that $S = \emptyset$. This implies that $\mathbf{a}_{j_0} = \mathbf{0}$. Now observe that $\mathbf{a}_j$ and $\mathbf{a}_{j'}$ are mutually distinct for all $j, j' \in [e]$, $j \neq j'$. Indeed, if they were equal then this would imply that $R_j = R_{j'}$. Hence, $\mathsf{supp}(\mathbf{a}_j) \neq \emptyset$ for any $j \neq j_0$. We note that $n_j = m_j$ for all $j \neq j_0$ by the maximality of S. Hence, $n_{j_0} = n - \sum_{j\neq j_0} n_j = n - \sum_{j\neq j_0} m_j = m_{j_0}$, contradicting our assumption. Hence, $S \neq \emptyset$.

Consider $J := \{j \in [e] \mid \mathsf{supp}(\mathbf{a}_j) = S\}$. For each $j \in J$, consider the truncated vector $\hat{\mathbf{a}}_j := (a_{ij} \mid i \in S)$. We note that $\hat{\mathbf{a}}_j$, for $j \in J$, all have positive entries and are mutually distinct. Lemma 4.1 in Grohe [2020b] implies that we can find a vector (with non-zero entries) $\hat{\mathbf{s}} = (\hat{s}_i \mid i \in S)$ such that the numbers $\hat{\mathbf{a}}_j^{\hat{\mathbf{s}}}$ for $j \in J$ are mutually distinct as well. We next consider $\mathbf{s} = (s_1, \dots, s_K)$ with $s_i = \hat{s}_i$ if $i \in S$ and $s_i = 0$ otherwise. Then by definition of $\hat{\mathbf{s}}$, also $\mathbf{a}_j^{\mathbf{s}}$ for $j \in J$ are mutually distinct.

We next note that for every $p \in \mathbb{N}$, $\mathbf{a}_j^{p\mathbf{s}} = (\mathbf{a}_j^{\mathbf{s}})^p$ and if we define $\mathbf{A}$ to be the $|J| \times |J|$-matrix such that $A_{jj'} := \mathbf{a}_j^{j'\mathbf{s}}$ then this will be an invertible matrix (Vandermonde). We use this invertibility to show that $n_{j_0} = m_{j_0}$.

Let $\mathbf{n}_J := (n_j \mid j \in J)$ and $\mathbf{m}_J = (m_j \mid j \in J)$. If we inspect the j'th entry of $\mathbf{n}_J \cdot \mathbf{A}$, then this is equal to

$$\sum_{j\in J} n_j \mathbf{a}_j^{j'\mathbf{s}} = \sum_{j\in[e]} n_j \mathbf{a}_j^{j'\mathbf{s}} - \sum_{\substack{j\in[e] \\ S\not\subseteq\mathsf{supp}(\mathbf{a}_j)}} n_j \mathbf{a}_j^{j'\mathbf{s}} - \sum_{\substack{j\in[e] \\ S\subset\mathsf{supp}(\mathbf{a}_j)}} n_j \mathbf{a}_j^{j'\mathbf{s}}.$$

We want to reduce the above expression to

$$\sum_{j\in J} n_j \mathbf{a}_j^{j'\mathbf{s}} = \sum_{j\in[e]} n_j \mathbf{a}_j^{j'\mathbf{s}} - \sum_{\substack{j\in[e]\\ S\subset \mathsf{supp}(\mathbf{a}_j)}} n_j \mathbf{a}_j^{j'\mathbf{s}}.$$

To see that this holds, we verify that when $S \not\subseteq \mathsf{supp}(\mathbf{a}_j)$ then $\mathbf{a}_j^{j'\mathbf{s}} = 0$. Indeed, take an $\ell \in S$ such that $\ell \notin \mathsf{supp}(\mathbf{a}_j)$. Then, $\mathbf{a}_j^{j'\mathbf{s}}$ contains the factor $a_{\ell j}^{j' s_\ell} = 0^{s_\ell}$ with $s_\ell = \hat{s}_\ell \neq 0$. Hence, $\mathbf{a}_j^{j'\mathbf{s}} = 0$.

Now, by the maximality of S, for all j with $S \subset \mathsf{supp}(\mathbf{a}_j)$ we have $n_j = m_j$ and thus

$$\sum_{\substack{j\in[e]\\ S\subset \mathsf{supp}(\mathbf{a}_j)}} n_j \mathbf{a}_j^{j'\mathbf{s}} = \sum_{\substack{j\in[e]\\ S\subset \mathsf{supp}(\mathbf{a}_j)}} m_j \mathbf{a}_j^{j'\mathbf{s}}.$$

Since $\sum_{j\in[e]} n_j \mathbf{a}_j^{j'\mathbf{s}} = \sum_{j\in[e]} m_j \mathbf{a}_j^{j'\mathbf{s}}$, we thus also have that

$$\sum_{j\in J} n_j \mathbf{a}_j^{j'\mathbf{s}} = \sum_{j\in J} m_j \mathbf{a}_j^{j'\mathbf{s}}.$$

Since this holds for all $j' \in J$, we have $\mathbf{n}_J \cdot \mathbf{A} = \mathbf{m}_J \cdot \mathbf{A}$ and by the invertibility of $\mathbf{A}$, $\mathbf{n}_J = \mathbf{m}_J$. In particular, since $j_0 \in J$, $n_{j_0} = m_{j_0}$ contradicting our assumption.

As a consequence, $n_j = m_j$ for all $j \in [e]$ and thus we have our desired bijection.

It remains to verify that we only need a finite number of $\mathcal{F}$-pattern trees to conclude that $n_j = m_j$ for all $j \in [e]$. In fact, the above proof indicates that we just need to check test for each root label a, we need to check identities for the finite number of pattern trees used to define the matrix $\mathbf{A}$.

Proof of equivalence 2 This equivalence is shown just like proof of Theorem 4.4. in Grohe [2020a] with the additional techniques from Lemma 4.2 in Grohe [2020b].

$\boxed{\Longrightarrow}$ We first show that $G \equiv^{(d)}_{\mathcal{F}\text{-}\mathsf{WL}} H$ implies $\mathsf{hom}(T,G) = \mathsf{hom}(T,H)$ for unrooted $\mathcal{F}$-pattern trees T of depth at most d.

Assume that $V_X \cap V_Y = \emptyset$ for $X, Y \in \{G, H\}$. For $x \in V_X$ and $y \in V_Y$, define $x \sim_d y$ if and only if $\mathsf{hom}(T^r, X^x) = \mathsf{hom}(T^r, Y^y)$ for all $\mathcal{F}$-pattern trees T^r of depth at most d. Let $R_1, \ldots, R_e$ be the $\sim_d$-equivalence classes and for each $j \in [e]$, let $p_j := |R_j \cap V_G|$ and $q_j := |R_j \cap V_H|$. Suppose that $G \equiv^{(d)}_{\mathcal{F}\text{-}\mathsf{WL}} H$. This implies that $p_j = q_j$ for every $j \in [e]$.

Let T be an unrooted $\mathcal{F}$-pattern tree of depth at most d, let r be any vertex on the backbone of T, and let T^r be the rooted $\mathcal{F}$-pattern tree obtained from T by declaring r as its root. By definition, for $X \in \{G, H\}$, any $x \in V_X \cap R_j$, $\mathsf{hom}(T^r, X^x)$ are all the same number, only dependent on $j \in [e]$. Hence,

$$\begin{aligned}\mathsf{hom}(T,G) &= \sum_{v\in V(G)} \mathsf{hom}(T^r, G^v) = \sum_{j\in[e]} p_j \mathsf{hom}(T^r, G^{v_j}) \\ &= \sum_{j\in[e]} q_j \mathsf{hom}(T^r, H^{w_j}) = \sum_{w\in V(H)} \mathsf{hom}(T^r, H^w) = \mathsf{hom}(T,H),\end{aligned}$$

where v_j and w_j are arbitrary vertices in $R_j \cap V_G$ and $R_j \cap V_H$, respectively, and where we used that $\mathsf{hom}(T^r, G^{v_j}) = \mathsf{hom}(T^r, H^{w_j})$ and $p_j = q_j$. Since this holds for any unrooted $\mathcal{F}$-pattern tree T of depth at most d, we have show the desired implication.

$\boxed{\Longleftarrow}$ We next check the other direction. That is, we assume that $\mathsf{hom}(T,G) = \mathsf{hom}(T,H)$ holds for any unrooted $\mathcal{F}$-pattern tree T of depth at most d and verify that $G \equiv^{(d)}_{\mathcal{F}\text{-}\mathsf{WL}} H$.

For $x \sim_d y$ to hold for $x \in V_X$, $y \in V_Y$ and $X, Y \in \{G, H\}$, we earlier showed that this corresponds to checking whether $\mathsf{hom}(T_i^{r_i}, X^x) = \mathsf{hom}(T_i^{r_i}, Y^y)$ for a *finite* number K rooted $\mathcal{F}$-pattern trees $T_i^{r_i}$. By definition of the R_j's, $a_{ij} := \mathsf{hom}(T_i^{r_i}, X^x)$ for $x \in R_j$ is well-defined (independent of the choice of $X \in \{G, H\}$ $x \in V_X$). For the rooted $T_i^{r_i}$'s we denote by T_i its unrooted version. Similarly as before,

$$\mathsf{hom}(T_i, G) = \sum_{j\in[e]} a_{ij} p_j = \sum_{j\in[e]} a_{ij} q_j = \mathsf{hom}(T_i, H).$$

We next show that $p_j = q_j$ for $j \in [e]$. In fact, this is shown in precisely the same way as in our previous characterisation and based on Lemma 4.2 in Grohe [2020b]. That is, we again consider trees obtained by joining copies of the T_i's, to obtain, for compatible $\mathbf{s} \in \mathbb{N}^K$,

$$\sum_{j\in[e]} a_{ij}^{s_i} p_j = \sum_{j\in[e]} a_{ij}^{s_i} q_j.$$

It now suffices to repeat the same argument as before (details omitted). □

B Proofs of Section 4

B.1 Additional details of standard concepts

Core and treewidth. A graph G is a *core* if all homomorphisms from G to itself are injective. The *treewidth* of a graph $G = (V, E, \chi)$ is a measure of how much G resembles a tree. This is defined in terms of the *tree decompositions* of G, which are pairs (T, λ), for a tree $T = (V_T, E_T)$ and λ a mapping that associates each vertex t of V_T with a set $\lambda(t) \subseteq V$, satisfying the following:

- The union of $\lambda(t)$, for $t \in V_T$, is equal to V;
- The set $\{t \in V_T \mid v \in \lambda(t)\}$ is connected, for all $v \in V$; and
- For each $\{u, v\} \in E$ there is $t \in V_T$ with $\{u, v\} \in \lambda(t)$.

The *width* of (T, λ) is $\min_{t\in T}(|\lambda(t)|) - 1$. The treewidth of G is the minimum width of its tree decompositions. For instance, trees have treewidth one, cycles have clique two, and the k-clique K_k has treewidth $k - 1$ (for $k > 1$).

If P^r is a pattern, then its treewidth is defined as the treewidth of the graph P. Similarly, P^r is a core if P is.

***k*-WL.** A *partial isomorphism* from a graph G to a graph H is a set $\pi \subseteq V_G \times V_H$ such that all $(v, w), (v', w') \in \pi$ satisfy the equivalences $v = v' \Leftrightarrow w = w'$, $\{v, v'\} \in E_G \Leftrightarrow \{w, w'\} \in E_H$, $\chi_G(v) = \chi_H(w)$ and $\chi_G(v') = \chi_H(w')$. We may view π as a bijective mapping from a subset $X \subseteq V_G$ to a subset of $Y \subseteq V_H$ that is an isomorphism from the induced subgraph $G[X]$ to the induced subgraph $H[Y]$. The *isomorphism type* $\mathsf{isotp}(G, \bar{v})$ of a k-tuple $\bar{v} = (v_1, \ldots, v_k)$ is a label in some alphabet Σ such that $\mathsf{isotp}(G, \bar{v}) = \mathsf{isotp}(H, \bar{w})$ if and only if $\pi = \{(v_1, w_1), \ldots, (v_k, w_k)\}$ is a partial isomorphism from G to H.

Let $k \geq 1$ and $G = (V, E, \chi)$. The k-dimensional Weisfeiler-Leman algorithm (k-WL) computes a sequence of labellings $\chi_{k,G}^{(d)}$ from $V^k \to \Sigma$. We denote by $\chi_{k,G,\bar{v}}^{(d)}$ the label assigned to the k-tuple $\bar{v} \in V^k$ in round d. The initial labelling $\chi_{k,G}^{(0)}$ assigns to each k-tuple $\bar{v}$ is isomorphism type $\mathsf{isotp}(G, \bar{v})$. Then, for round d,

$$\chi_{k,G,\bar{v}}^{(d)} := \big(\chi_{k,G,\bar{v}}^{(d-1)}, M_{\bar{v}}^{(d-1)}\big),$$

where $M_{\bar{v}}^{(d-1)}$ is the multiset

$$\Big\{\!\!\Big\{ \big(\mathsf{isotp}(v_1, \ldots, v_k, w), \chi_{k,G,(v_1,\ldots,v_{k-1},w)}^{(d-1)}, \chi_{k,G,(v_1,\ldots,v_{k-2},w,v_k)}^{(d-1)}, \ldots, \chi_{k,G,(w,v_2,\ldots,v_k)}^{(d-1)}\big) \Big| \; w \in V \Big\}\!\!\Big\}.$$

As observed in Dell et al. [2018], if $k \geq 2$ holds, then we can omit the entry $\mathsf{isotp}(v_1, \ldots, v_k, w)$ from the tuples in $M_{\bar{v}}$, because all the information it contains is also contained in the entries $\chi_{k,G,\ldots}^{(d-1)}$ of these tuples. Also, $\mathsf{WL} = 1$-WL in the sense that $\chi_{G,v}^{(d)} = \chi_{G,v'}^{(d)}$ if and only if $\chi_{1,G,v}^{(d)} = \chi_{1,G,v'}^{(d)}$ for all $v, v' \in V$. The k-WL algorithm is run until the labelings stabilises, i.e., if for all $\bar{v}, \bar{w} \in V^k$, $\chi_{k,G,\bar{v}}^{(d)} = \chi_{k,G,\bar{w}}^{(d)}$ if and only if $\chi_{k,G,\bar{v}}^{(d+1)} = \chi_{k,G,\bar{w}}^{(d+1)}$. We say that k-WL *distinguishes two graphs G and H* if the multisets of labels for all k-tuples of vertices in G and H, respectively, coincides. Similar notions as are place for distinguishing k-tuples, and for distinguishing graphs (or vertices) based on labels computed by a given number of rounds.

We remark that k-WL algorithm given here is sometimes referred to as the "folklore" version of the k-dimensional Weisfeiler-Leman algorithm. It is known that indistinguishability of graphs by k-WL is equivalent to indistinguishability by sentences in the the $k+1$-variable fragment of first order logic with counting Cai et al. [1992], and to $\mathsf{hom}(P, G) = \mathsf{hom}(P, H)$ for every graph of treewidth k Dvorak [2010], Dell et al. [2018].

B.2 Proof of Proposition 3

We show that for each finite set $\mathcal{F}$ of patterns, the expressive power of $\mathcal{F}$-WL is bounded by k-WL, where k is the largest treewidth of a pattern in $\mathcal{F}$.

We first recall the following characterisation of k-WL-equivalence Dvorak [2010], Dell et al. [2018]. For any two graphs G and H,

$$G \equiv_{k\text{-WL}} H \iff \mathsf{hom}(P, G) = \mathsf{hom}(P, H)$$

for every graph P of treewidth at most k. On the other hand, we know from Theorem 1 that

$$G \equiv_{\mathcal{F}\text{-WL}} H \iff \mathsf{hom}(T, G) = \mathsf{hom}(T, H)$$

for every $\mathcal{F}$-pattern tree T. Hence, we may conclude that

$$G \equiv_{k\text{-WL}} H \implies G \equiv_{\mathcal{F}\text{-WL}} H$$

if we can show that any $\mathcal{F}$-pattern tree has treewidth at most k.

Suppose that k is the maximal treewidth of a pattern in $\mathcal{F}$. To conclude the proof, we verify that the treewidth of any $\mathcal{F}$-pattern tree is bounded by k.

Lemma 1. *If k is the maximal treewidth of a pattern in $\mathcal{F}$, then the treewidth of any $\mathcal{F}$-pattern tree T is bounded by k.*

Proof. The proof is by induction on the number of patterns joined at any leaf of T. Clearly, if no patterns are joined, then T is simply a tree and its treewidth is 1. Otherwise, consider a $\mathcal{F}$-pattern tree $T = (V, E, \chi)$ whose treewidth is at most k, and a pattern P^r of treewidth k that is to be joined at vertex t of T. By the induction hypothesis, there is a decomposition (H, λ) for T witnessing its bounded treewidth, that is,

1. The union of all $\lambda(h)$, for $h \in V_H$, is equal to V;
2. The set $\{h \in V_H \mid t \in \lambda(h)\}$ is connected, for all $t \in V$;
3. For each $\{u, v\} \in E$ there is $h \in V_H$ with $\{u, v\} \in \lambda(h)$; and
4. The size of each set $\lambda(h)$ is at most $k + 1$.

Likewise, by assumption, for pattern P^r we have such a tree decomposition, say (H^P, λ^P).

Now consider any vertex h of the decomposition of T such that $\lambda(h)$ contains vertex t in T to which P^r is to be joined at its root. We can create a joint tree decomposition for the join of P^r and T (at node t) by merging H and H^P with an edge from vertex h in H to the root of H^P (recall H^P is a tree by definition). It is readily verified that this decomposition maintains all necessary properties. Indeed, condition 1 is clearly satisfied since λ and λ^p combined cover all vertices of the join of T with P^r. Furthermore, since the only node shared by T and P^r is the join node, and we merge H and H^P by putting an edge from node h in H to the root of H^P, connectivity of is guaranteed and condition 2 is satisfied. Moreover, since the operation of joining T and P^r does not create any extra edges, condition 2 is immediately verified, and so is 3, because we do not create any new vertices, neither in H nor in H^P, and we already know that λ and λ^P are bounded by $k + 1$. ☐

B.3 Proof of Theorem 3

We show that if $\mathcal{F}$ contains a pattern P^r which is a core and has treewidth k, then $\mathcal{F}$-WL is not bounded by $(k-1)$-WL. In other words, we construct two graphs G and H that can be distinguished by $\mathcal{F}$-WL but not by $(k-1)$-WL. It suffices to find such graphs that can be distinguished by $\{P^r\}$-WL but not by $(k-1)$-WL. The proof relies on the characterisation of $(k-1)$-WL indistinguishability in terms of the k-variable fragment C^k of first logic with counting and of k-pebble bijective games in particular Cai et al. [1992], Hella [1996]. More precisely, $G \equiv_{(k-1)\text{-WL}} H$ if and only if no sentence in C^k can distinguish G from H. In other words, for any sentence φ in C^k, $G \models \varphi$ if and only if $H \models \varphi$. We denote indistinguishability by C^k by $G \equiv_{\mathsf{C}^k} H$. We heavily rely on the constructions used in Atserias et al. [2007] and Bova and Chen [2019]. In fact, we show that the graphs G and H constructed in those works, suffice for our purpose, by extending their strategy for the k-pebble game to k-pebble bijective games.

Construction of the graphs G and H. Let P^r be a pattern in $\mathcal{F}$ which is a core and has treewidth k. For a vertex $v \in V_P$, we gather all its edges in $E_v := \big\{\{v, v'\} \mid \{v, v'\} \in E_P\big\}$. Let v_1 be one of the vertices in V_P.

For G, as vertex set V_G we take vertices of the form (v, f) with $v \in V_P$ and $f : E_v \to \{0, 1\}$. We require that

$$\sum_{e \in E_{v_1}} f(e) \mod 2 = 1 \text{ and } \sum_{e \in E_v} f(e) \mod 2 = 0 \text{ for } v \neq v_1, v \in V_P.$$

For H, as vertex set V_H we take vertices of the form (v, f) with $v \in V_P$ and $f : E_v \to \{0, 1\}$. We require that $\sum_{e \in E_v} f(e) \mod 2 = 0$, for all $v \in V_P$. We observe that G and H have the same number of vertices.

The edge sets E_G and E_H of G and H, respectively, are defined as follows: (v, f) and (v', f') are adjacent if and only if $v \neq v'$ and furthermore,

$$f(\{v, v'\} = f'(\{v, v'\}).$$

It is known that $\mathsf{hom}(P, G) = 0$ (here it is used that P is a core), $\mathsf{hom}(P, H) \neq 0$ and G and H are indistinguishably by means of sentences in the k-variable fragment FO^k of first order logic Atserias et al. [2007], Bova and Chen [2019]. To show our theorem, we thus need to verify that $G \equiv_{\mathsf{C}^k} H$ as well. Indeed, for if this holds, then $G \equiv_{(k-1)\text{-}\mathsf{WL}} H$ yet $G \not\equiv^{(0)}_{\{P\}\text{-}\mathsf{WL}} H$. Indeed, Theorem 1 implies that for $G \not\equiv^{(0)}_{\{P\}\text{-}\mathsf{WL}} H$ to hold, $\mathsf{hom}(P, G) = \mathsf{hom}(P, H)$, which we know not to be true. Hence, $G \not\equiv_{\{P\}\text{-}\mathsf{WL}} H$, as desired.

Showing C^k-indistinguishability of G and H. We next show that the graphs G and H are indistinguishable by sentences in C^k. This will be shown by verifying that the Duplicator has a winning strategy for the k-pebble bijective game on G and H [Hella, 1996].

The k-pebble bijective game. We recall that the k-pebble bijective game is played between two players, the Spoiler and the Duplicator, each placing at most k pebbles on the vertices of G and H, respectively. The game is played in a number of rounds. The pebbles placed after round r are typically represented by a partial function $p^{(r)} : \{1, \dots, k\} \to V_G \times V_H$. When $p^{(r)}(i)$ is defined, say, $p^{(r)}(i) = (v, w)$, this means that the Spoiler places the ith pebble on vertex v and the Duplicator places the ith pebble on w. Initially, no pebbles are placed on G and H and hence $p^{(0)}$ is undefined everywhere.

Then in round $r > 0$, the game proceeds as follows:

1. The Spoiler selects a pebble i in $[k]$. All other already placed pebbles are kept on the same vertices. We define $p^{(r)}(j) = p^{(r-1)}(j)$ for all $j \in [k]$, $j \neq i$.
2. The Duplicator responds by choosing a bijection $h : V_G \to V_H$. This bijection should be *consistent* with the pebbles in the restriction of $p^{(r-1)}$ to $[k] \setminus \{i\}$. That is, for every $j \in [k]$, $j \neq i$, if $p^{(r-1)}(j) = (v, w)$ then $w = h(v)$.
3. Next, the Spoiler selects an element $v \in V_G$.
4. The Duplicator defines $p^{(r)}(i) = (v, h(v))$. Hence, after this round, the ith pebble is placed on v by the Spoiler and on $h(v)$ by the Duplicator.

Let $\mathsf{dom}(p^{(r)})$ be the elements in $[k]$ for which $p^{(r)}$ is defined. For $i \in \mathsf{dom}(p^{(r)})$ denote by $(v_i, w_i) \in V_G \times V_H$ the pair of vertices on which the ith pebble is placed. The Duplicator *wins* round r if the mapping $v_i \mapsto w_i$ is partial isomorphism between G and H. More precisely, it should hold that for all edges $\{v_i, v_j\} \in E_G$ if and only if $(w_i, w_j) \in E_H$. In this case, the game continues to the next round. Infinite games are won by the Duplicator. A winning strategy consists of defining a bijection in step 2 in each round, allowing the game to continue, irregardless of which vertex v the Spoiler places a pebble in Step 3.

Winning strategy. We will now provide a winning strategy for the k-bijective game on our constructed graphs G and H. We recall that V_G and V_H have the same number of vertices, so a bijection between V_G and V_H exists. We show how the Duplicator can select a "good" bijection in Step 2 of the game, by induction on the number of rounds.

To state our induction hypothesis, we first recall some notions and properties from Atserias et al. [2007] and Bova and Chen [2019].

Let W be a walk in P and let e be an edge in E_P. Then, $\mathsf{occ}_W(e)$ denotes the number of occurrences of the edge e in the walk. More precisely, if $W = (a_1, \ldots, a_\ell)$ is a walk in P of length ℓ, then

$$\mathsf{occ}_W(e) := |\{i \in [\ell-1] \mid e = \{a_i, a_{i+1}\}\}|.$$

Furthermore, for a subset $S \subseteq V_P$, we define

$$\mathsf{avoid}(S) := \bigcup_{\{M \in \mathcal{M}, M \cap S = \emptyset\}} M,$$

where $\mathcal{M}$ is an arbitrary bramble of P of order $> k$. A bramble $\mathcal{M}$ is a set of *connected* subsets of V_P such that for any two elements M_1 and M_2 in $\mathcal{M}$, either $M_1 \cap M_2 \neq \emptyset$, or there exists a vertex $a \in M_1$ and $b \in M_2$ such that $\{a, b\} \in E_P$. The order of a bramble is the minimum size of a hitting set for $\mathcal{M}$. It is known that P has treewidth $\geq k$ if and only if it has a bramble of order $> k$. In what follows, we let $\mathcal{M}$ be any such bramble.

Lemma 2 (Lemma 14 in Bova and Chen [2019])**.** For any $1 \leq \ell \leq k$, let $(a_1, f_1), \ldots, (a_\ell, f_\ell)$ be vertices in V_G. Let W be a walk in P from v_1 to $\mathsf{avoid}(\{a_1, \ldots, a_\ell\})$. For all $i \in [\ell]$, let $f'_i : E_{a_i} \to \{0, 1\}$ be defined by

$$f'_i(e) = f_i(e) + \mathsf{occ}_W(e) \mod 2$$

for all $e \in E_{a_i}$. Then, the mapping $(a_i, f_i) \mapsto (a_i, f'_i)$, for all $i \in [\ell]$, is a partial isomorphism from G to H. □

We use this lemma to show that the bijection (to be defined shortly) selected by the Duplicator induces a partial isomorphism between G and H on the pebbled vertices.

We can now state our induction hypothesis: In each round r, there exists a bijection $h : V_G \to V_H$ which is

(a) consistent with the pebbles in the restriction of $p^{(r-1)}$ to $[k] \setminus \{i\}$ (Recall, Pebble i is selected by the Spoiler in Step 1.)

(b) If $p^{(r)}(j) = (a_j, f_j, h(a_j, f_j))$ for $j \in \mathsf{dom}(p^{(r)})$, then there exists a walk $W^{(r)}$ in P, from v to $\mathsf{avoid}(\{a_j \mid j \in \mathsf{dom}(p^{(r)})\}$, such that

$$h(a_j, f_j) = (a_j, f'_j),$$

where $f'_j(e) = f_j(e) + \mathsf{occ}_{W^{(r)}}(e) \mod 2$ for every $e \in E_{a_j}$. In other words, on the vertices in V_G pebbled by $p^{(r)}$, the bijection h is, by the previous Lemma, a partial isomorphism from G to H.

If this holds, then the strategy for the Duplicator is selecting that bijection h in each round.

Verification of the induction hypothesis. We assume that the special vertex v_1 in P has at least two neighbours. Such a vertex exists since otherwise P consists of a single edge while we assume P to be of treewidth at least two.

Base case. For the base case ($r = 0$) we define two walks: $W_1 = v_1, v_2$ and $W_2 = v_1, t$ with $v_2 \neq t$ and v_2, t are neighhbours of v_1. We define $h(a_i, f) = (a_i, f')$ with $f'(e) = f(e) + \mathsf{occ}_{W_1}(e) \mod 2$ if $a_i \neq t$, and $h(t, f) = (t, f')$ with $f'(e) = f(e) + \mathsf{occ}_{W_2}(e) \mod 2$.

The mapping h is a bijection from V_G to V_H. We note that it suffices to show that h is injective since V_G and V_H contain the same number of vertices. Since $h(a_i, f_i) \neq h(a_j, f_j)$ whenever $a_i \neq a_j$, we can focus on comparing $h(a_i, f)$ and $h(a_i, g)$ with $f \neq g$. This implies that $f(e) \neq g(e)$ for at least one edge $e \in N_{a_i}$. Clearly, this implies that $f'(e) = f(e) + \mathsf{occ}_W(e) \mod 2 \neq g'(e) = g(e) + \mathsf{occ}_W(e) \mod 2$. In fact this, holds for any walk W and thus in particular for W_1 and W_2. We further observe that h is consistent simply because no pebbles have been placed yet. For the same reason we can take the walk $W^{(0)}$ to be either W_1 or W_2.

Inductive case. Assume that the induction hypothesis holds for round r and consider round $r + 1$. Let $p^{(r)} = (a_j, f_j, a_j, f'_j)$ for $j \in \mathsf{dom}(p^{(r)})$. By induction, there exists a bijection $h' : V_G \to V_H$ such that $h(a_j, f_j) = (a_j, f'_j)$ and furthermore, $f'_j(e) = f_j(e) + \mathsf{occ}_{W^{(r)}}(e) \mod 2$ for every $e \in N_{a_j}$, for some walk $W^{(r)}$ from v_1 to $t \in \mathsf{avoid}(\{a_j \mid j \in \mathsf{dom}(p^{(r)})\})$.

Assume that the Spoiler selects $i \in [k]$ in Step 1 in round $r + 1$. We define the Duplicator's bijection $h : V_G \to V_H$ for round $r + 1$, as follows. Recall that $t \in V_P$ is the vertex in which the walk $W^{(r)}$ ends.

- For all $(a, f) \in V_G$ such that $a \neq t$, we define $h(a, f) = (a, f')$ where for each $e \in E_a$:
$$f'(e) = f(e) + \mathsf{occ}_{W^{(r)}}(e) \mod 2.$$
- For all $(t, f) \in V_G$, we will extend $W^{(r)}$ with a walk W' so that it ends in a vertex t' different from t. Suppose that $M \in \mathcal{M}$ such that $t \in M$. We want to find an $M' \in \mathcal{M}$ such that $M' \cap (\{a_j \mid j \in \mathsf{dom}(p^{(r)}), j \neq i\} \cup \{t\}) = \emptyset$. We can then take t' to be a vertex in M' and since M and M' are both connected, and either have a vertex in common or an edge between them, we can let W' be a walk from t to t' entirely in M and M'. Now, such an M' exists since otherwise $\{a_j \mid j \in \mathsf{dom}(p^{(r)}), j \neq i\} \cup \{t\}$ would be a hitting set for $\mathcal{M}$ of size at most k. We know, however, that any hitting set $\mathcal{M}$ must be of size $k + 1$ because of the treewidth k assumption for P. We now define the bijection as $h(t, f) = (t, f')$ where for each $e \in E_t$:
$$f'(e) = f(e) + \mathsf{occ}_{W^{(r)},W'}(e) \mod 2.$$

This concludes the definition of $h : V_G \to V_H$. We need to verify a couple of things: (i) h is bijection; (ii) h is consistent with all pebbles in $p^{(r)}$ except for the "unpebbled" one $p^{(r)}(i)$; and (iii) it induces a partial isomorphism on pebbled vertices.

(i) h is a bijection. Since V_G and V_H are of the same size, it suffices to show that h is an injection. Clearly, $h(a_1, f_1) \neq h(a_2, f_2)$ whenever $a_1 \neq a_2$. We can thus focus on $h(a, f_1)$ and $h(a, f_2)$ with $f_1 \neq f_2$. Then, f_1 and f_2 differ in at least one edge $e \in E_a$ and for this edge:
$$f'_1(e) = f_1(e) + \mathsf{occ}_W(e) \mod 2 \neq f_2(e) + \mathsf{occ}_W(e) \mod 2 = f'_2(e).$$
for any walk W. In particular, this holds for both walks used in the definition of h: $W^{(r)}$, used when $a \neq t$, and $W^{(r)}, W'$ used when $a = t$. Hence, h is indeed a bijection.

(ii) h is consistent. For each $j \in \mathsf{dom}(p^{(r+1)})$ with $j \neq i$, let $p^{(r+1)} = (a_j, f_j, a_j, f'_j)$. Now, by induction, $W^{(r)}$ ended in a vertex t distinct from any of these a_j's and thus none of these a_j's are equal to t. This implies that $h(a_j, f_j) = (a_j, f''_j)$ with $f''_j(e) = f_j(e) + \mathsf{occ}_{W^{(r)}}(e) \mod 2$. But this is precisely how $p^{(r)}$ placed its pebbles, by induction. Hence, $f''_j(e) = f'_j(e)$ and thus h is consistent.

(iii) $p^{(r+1)}$ induces a partial isomorphism. After the Spoiler picked an element $(a_i, f_i) \in V_G$, we now know that $p^{(r+1)}(j) = (a_j, f_j, h(a_j, f_j))$ for all $j \in \mathsf{dom}(p^{(r+1)})$. We recall that h is defined in two possible ways, using two distinct walks: $W^{(r)}$, for vertices in V_G not involving t, or, otherwise using the walk $W^{(r)}, W'$, for vertices in V_G involving t.

Hence, when all a_j's for $p^{(r+1)}$ are distinct from t, then $h(a_j, f_j) = (a_j, f'_j)$ with $f'_j(e) = f_j(e) + \mathsf{occ}_{W^{(r)}}(e) \mod 2$ and we can simply take the new walk $W^{(r+1)}$ to be $W^{(r)}$. Then, Lemma 2 implies that the mapping $(a_j, f_j) \to h(a_j, f_j)$, for $j \in \mathsf{dom}(p^{(r+1)})$ is a partial isomorphism from G to H, as desired.

Otherwise, we know that $a_j \neq t$ for $j \neq i$ but $a_i = t$. That is, the Spoiler places the ith pebble on a vertex of the form (t, f) in V_G. We now have that h is defined in two ways for the pebbled elements using the two distinct walks. We next show that $W^{(r)}, W'$ can be used for both types of pebbled elements in $p^{(r+1)}$, those of the form (a_j, f) with $a_j \neq t$ and (t, f). For the last type this is obvious since we defined $h(t, f)$ in terms of $W^{(r)}, W'$. For the former type, we note that $a_j \notin M$ and $a_j \notin M'$ for $j \neq i$. If we take an edge $e \in N_{a_j}$, then $\mathsf{occ}_{W^r,W'}(e) = \mathsf{occ}_{W^{(r)}}(e)$ because W' lies entirely in M and M'. As a consequence, for (a_j, f_j) with $j \neq i$, for all $e \in N_j$:
$$f'_j(e) = f_j(e) + \mathsf{occ}_{W^{(r)}}(e) \mod 2$$

$$= f_j(e) + \mathsf{occ}_{W^{(r)},W'}(e) \mod 2.$$

Then, Lemma 2 implies that the mapping $(a_j, f_j) \to h(a_j, f_j)$, for $j \in \mathsf{dom}(p^{(r+1)})$ is a partial isomorphism from G to H, because we can use the same walk $W^{(r),W'}$ for all pebbled vertices.

B.4 Proof of Proposition 4

We show that no finite set $\mathcal{F}$ of patterns suffices for $\mathcal{F}$-WL to be equivalent to k-WL, for $k > 1$, in terms of expressive power. The proof is by contradiction. That is, suppose that there exists a set $\mathcal{F}$ such that $G \equiv_{\mathcal{F}\text{-WL}} H \Leftrightarrow G \equiv_{k\text{-WL}} H$ for any two graphs G and H. In particular, $G \equiv_{\mathcal{F}\text{-WL}} H \Rightarrow G \equiv_{k\text{-WL}} H$ and thus also $G \equiv_{\mathcal{F}\text{-WL}} H \Rightarrow G \equiv_{2\text{-WL}} H$, since the 2-WL-test is upper bounded by any k-WL-test for $k > 2$. We argue that no finite set $\mathcal{F}$ exists satisfying $G \equiv_{\mathcal{F}\text{-WL}} H \Rightarrow G \equiv_{2\text{-WL}} H$.

Let m denote the maximum number of vertices of any pattern in $\mathcal{F}$.[5] Furthermore, consider graphs G and H, where G is the disjoint union of $m+2$ copies of the cycle C_{m+1}, and H is the union of $m+1$ copies of the cycle C_{m+2}. Note that G and H have the same number of vertices.

We observe that any homomorphism from a pattern P^r in $\mathcal{F}$ to G^v or H^w, for vertices $v \in V_G$ and $w \in V_H$, maps P^r to either a copy of C_{m+1} (for G) or a copy of C_{m+2} (for H). Furthermore, any such homomorphism maps P^r in a subgraph of C_{m+1} or C_{m+2}, consisting of at most m vertices. There is, however, a unique (up to isomorphism) subgraph of m vertices in C_{m+1} and C_{m+2}. Indeed, such subgraphs will be a path of length m. This implies that $\mathsf{hom}(P^r, G^v) = \mathsf{hom}(P^r, H^w)$ for any $v \in V_G$ and $w \in V_H$. Since the argument holds for any pattern P^r in $\mathcal{F}$, all vertices in G and H will have the same homomorphism count for patterns in $\mathcal{F}$. Furthermore, since both G and H are regular graphs (each vertex has degree two), this implies that $\mathcal{F}$-WL cannot distinguish between G and H. This is formalised in the following lemma. We recall that a t-regular graph is a graph in which every vertex has degree t.

Lemma 3. *For any set $\mathcal{F}$ of patterns and any two t-regular (unlabelled) graphs G and H such that $\mathsf{hom}(P^r, X^x) = \mathsf{hom}(P^r, Y^y)$ for $P^r \in \mathcal{F}$, $X, Y \in \{G, H\}$, $x \in V_X$ and $y \in V_Y$ holds, $G \equiv_{\mathcal{F}\text{-WL}} H$.*

Proof. The lemma is readily verified by induction on the number d of rounds of $\mathcal{F}$-WL. We show a stronger result in that $\chi^{(d)}_{\mathcal{F},X,x} = \chi^{(d)}_{\mathcal{F},Y,y}$ for any d, $X, Y \in \{G, H\}$, $x \in V_X$ and $y \in V_Y$, from which $G \equiv_{\mathcal{F}\text{-WL}} H$ follows. By our Theorem 1, it suffices to show that $\mathsf{hom}(T^r, X^x) = \mathsf{hom}(T^r, Y^y)$ for $\mathcal{F}$-pattern trees of depth at most d. Let $\mathcal{F} = \{P^r_1, \ldots, P^r_\ell\}$. For the base case, let T^r be a join pattern $\mathcal{F}^{\mathbf{s}}$ for some $\mathbf{s} = (s_1, \ldots, s_\ell) \in \mathbb{N}^\ell$. Then,

$$\mathsf{hom}(T^r, X^x) = \prod_{i=1}^{\ell} (\mathsf{hom}(P^r_i, X^x))^{s_i} = \prod_{i=1}^{\ell} (\mathsf{hom}(P^r_i, Y^y))^{s_i} = \mathsf{hom}(T^r, Y^y),$$

since $\mathsf{hom}(P^r_i, X^x) = \mathsf{hom}(P^r_i, Y^y)$ for any $P^r_i \in \mathcal{F}$. Then, for the inductive case, assume that $\mathsf{hom}(S^r, X^x) = \mathsf{hom}(S^r, Y^y)$ for any $\mathcal{F}$-pattern tree S^r of depth at most $d-1$, $X, Y \in \{G, H\}$, $x \in V_X$ and $y \in V_Y$, and consider an $\mathcal{F}$-pattern T^r of depth d. Let $S^{c_1}_1, \ldots, S^{c_p}_p$ be the $\mathcal{F}$-pattern trees of depth at most $d-1$ rooted at the children $c_1, \ldots, c_p$ of r in the backbone of T^r. As before, let $\mathcal{F}^{\mathbf{s}}$ the pattern joined at r in T^r. Then,

$$\begin{aligned}
\mathsf{hom}(T^r, X^x) &= \mathsf{hom}(\mathcal{F}^{\mathbf{s}}, X^x) \prod_{i=1}^{p} \sum_{x' \in N_X(x)} \mathsf{hom}(S^{c_i}_i, X^{x'}) = \mathsf{hom}(\mathcal{F}^{\mathbf{s}}, X^x) \prod_{i=1}^{p} t \cdot \mathsf{hom}(S^{c_i}_i, X^{\tilde{x}}) \\
&= \mathsf{hom}(\mathcal{F}^{\mathbf{s}}, Y^y) \prod_{i=1}^{p} t \cdot \mathsf{hom}(S^{c_i}_i, Y^{\tilde{y}}) = \mathsf{hom}(\mathcal{F}^{\mathbf{s}}, Y^y) \prod_{i=1}^{p} \sum_{y' \in N_Y(y)} \mathsf{hom}(S^{c_i}_i, Y^{y'}) \\
&= \mathsf{hom}(T^r, Y^y),
\end{aligned}$$

[5] Strictly speaking, we can use the diameter of any pattern in $\mathcal{F}$ instead, but it is easier to convey the proof simply by taking number of vertices.

where we used that $N_X(x)$ and $N_Y(y)$ both consists of t vertices (regularity), by the induction hypothesis all vertex have the same homomorphism counts for $\mathcal{F}$-patterns trees of depth at most $d-1$, and where $\tilde{x}$ and $\tilde{y}$ are taken to be arbitrary vertices in $N_X(x)$ and $N_Y(y)$, respectively. □

Hence, since G and H are 2-regular and satisfy the conditions of the lemma, we may indeed infer that $G \equiv_{\mathcal{F}\text{-WL}} H$. We note, however, that $G \not\equiv_{2\text{-WL}} H$. Indeed, from Dvorak [2010] and Dell et al. [2018] we know that $G \equiv_{2\text{-WL}} H$ implies that $\mathsf{hom}(P, G) = \mathsf{hom}(P, H)$ for any graph P of treewidth at most two. In particular, $G \equiv_{2\text{-WL}} H$ implies that $\mathsf{hom}(C_\ell, G) = \mathsf{hom}(C_\ell, H)$ for all cycles C_ℓ. We now conclude by observing that $\mathsf{hom}(C_{m+1}, G) \neq \mathsf{hom}(C_{m+1}, H)$ by construction. Recall that G consists of $m+2$ disjoint copies of C_{m+1} and H consists of $m+1$ copies of C_{m+2}. Consider $\mathsf{hom}(C_{m+1}, G)$ and $\mathsf{hom}(C_{m+1}, H)$. We can write these as $(m+2)(m+1)\mathsf{hom}(C^r_{m+1}, C^v_{m+1})$ and $(m+1)(m+2)\mathsf{hom}(C^r_{m+1}, C^w_{m+2})$ for some fixed vertices v and w and where all cycles are now rooted. It now suffices to observe that all homomorphisms h from C^r_{m+1} to C^w_{m+2} are such that the image $h(C^r_{m+1})$ contain $< m+1$ vertices. And moreover, with any such h, we can associate a unique h' from C^r_{m+1} to C^v_{m+1} (such that also $h'(C^r_{m+1})$ contains $< m+1$ vertices). Finally, we note that there are two homomorphisms from C^r_{m+1} to C^v_{m+1} which are surjections and thus cover all $m+1$ vertices in C^v_{m+1}. We may thus conclude that $\mathsf{hom}(C^r_{m+1}, C^w_{m+2}) < \mathsf{hom}(C^r_{m+1}, C^v_{m+1})$, from which we can infer that $\mathsf{hom}(C_{m+1}, G) \neq \mathsf{hom}(C_{m+1}, H)$, as desired. We have thus found two graphs with cannot be distinguished by $\mathcal{F}$-WL, but that can be distinguished by 2-WL, contradicting our assumption that $G \equiv_{\mathcal{F}\text{-WL}} H \Rightarrow G \equiv_{2\text{-WL}} H$.

C Proofs of Section 5

C.1 Proof of Proposition 5

We show that for any $k > 3$, $\{C^r_3, \ldots, C^r_k\}$-WL is more expressive than $\{C^r_3, \ldots, C^r_{k-1}\}$-WL. More precisely, we construct two graphs G and H such that G and H cannot be distinguished by $\{C^r_3, \ldots, C^r_{k-1}\}$-WL, but they can be distinguished by $\{C^r_3, \ldots, C^r_k\}$-WL.

The proof is analogous to the proof of Proposition 4. Indeed, it suffices to let G consist of k disjoint copies of C_{k+1} and H to consist of $k+1$ disjoint copies of C_k. Then, as observed in the proof of Proposition 4, G and H will be indistinguishable by $\{C^r_3, \ldots, C^r_{k-1}\}$-WL simply because each pattern has at most $k-1$ vertices. Yet, by construction, $\mathsf{hom}(C_k, G) \neq \mathsf{hom}(C_k, H)$ and thus G and H are distinguishable (already by the initial labelling) by $\{C^r_3, \ldots, C^r_k\}$-WL.

C.2 Proof of Proposition 6

Let $P^r = P^r_1 \star P^r_2$ be a pattern that is the join of two smaller patterns. We show that for any any set $\mathcal{F}$ of patterns, we have that $\mathcal{F} \cup \{P^r\}$-WL is upper bounded by $\mathcal{F} \cup \{P^r_1, P^r_2\}$-WL. That is, for every two graphs G and H, $G \equiv_{\mathcal{F}\cup\{P^r_1,P^r_2\}\text{-WL}} H$ implies $G \equiv_{\mathcal{F}\cup\{P^r\}\text{-WL}} H$. By definition, $G \equiv_{\mathcal{F}\cup\{P^r_1,P^r_2\}\text{-WL}} H$ is equivalent to $\{\!\{\chi^{(d)}_{\mathcal{F}\cup\{P^r_1,P^r_2\},G,v} \mid v \in V_G\}\!\} = \{\!\{\chi^{(d)}_{\mathcal{F}\cup\{P^r_1,P^r_2\},H,w} \mid w \in V_H\}\!\}$. In other words, with every $v \in V_G$ we can associate a unique $w \in V_H$ such that $\chi^{(d)}_{\mathcal{F}\cup\{P^r_1,P^r_2\},G,v} = \chi^{(d)}_{\mathcal{F}\cup\{P^r_1,P^r_2\},H,w}$. We show, by induction on d, that this implies that $\chi^{(d)}_{\mathcal{F}\cup\{P^r\},G,v} = \chi^{(d)}_{\mathcal{F}\cup\{P^r\},H,w}$. This suffices to conclude that $\{\!\{\chi^{(d)}_{\mathcal{F}\cup\{P^r\},G,v} \mid v \in V_G\}\!\} = \{\!\{\chi^{(d)}_{\mathcal{F}\cup\{P^r\},H,w} \mid w \in V_H\}\!\}$ and thus $G \equiv_{\mathcal{F}\cup\{P^t\}\text{-WL}} H$.

Base case. We show that $\{\!\{\chi^{(d)}_{\mathcal{F}\cup\{P^r_1,P^r_2\},G,v} \mid v \in V_G\}\!\} = \{\!\{\chi^{(d)}_{\mathcal{F}\cup\{P^r_1,P^r_2\},H,w} \mid w \in V_H\}\!\}$ implies that with every $v \in V_G$ we can associate a unique $w \in V_H$ satisfying $\chi^{(0)}_{\mathcal{F}\cup\{P^r\},G,v} = \chi^{(0)}_{\mathcal{F}\cup\{P^r\},H,w}$. Indeed, as already observed, $\{\!\{\chi^{(d)}_{\mathcal{F}\cup\{P^r_1,P^r_2\},G,v} \mid v \in V_G\}\!\} = \{\!\{\chi^{(d)}_{\mathcal{F}\cup\{P^r_1,P^r_2\},H,w} \mid w \in V_H\}\!\}$ implies that with every $v \in V_G$ we can associate a unique $w \in V_H$ such that $\chi^{(d)}_{\mathcal{F}\cup\{P^r_1,P^r_2\},G,v} = \chi^{(d)}_{\mathcal{F}\cup\{P^r_1,P^r_2\},H,w}$. This in turn implies that $\chi^{(0)}_{\mathcal{F}\cup\{P^r_1,P^r_2\},G,v} = \chi^{(0)}_{\mathcal{F}\cup\{P^r_1,P^r_2\},H,w}$, which implies that $\mathsf{hom}(P^r_1, G^v) = \mathsf{hom}(P^r_1, H^w)$ and $\mathsf{hom}(P^r_2, G^v) = \mathsf{hom}(P^r_2, H^w)$ and $\mathsf{hom}(Q^r, G^v) = \mathsf{hom}(Q^r, H^w)$ for every $Q^r \in \mathcal{F}$. As a consequence, from properties of the graph join operators, since $P^r = P^r_1 \star P^r_2$:

$$\mathsf{hom}(P^r, G^v) = \mathsf{hom}(P^r_1, G^v) \cdot \mathsf{hom}(P^r_2, G^v) = \mathsf{hom}(P^r_1, H^w) \cdot \mathsf{hom}(P^r_2, H^w) = \mathsf{hom}(P^r, H^w),$$

and thus also $\chi^{(0)}_{\mathcal{F}\cup\{P^r\},G,v} = \chi^{(0)}_{\mathcal{F}\cup\{P^r\},H,w}$.

Inductive case. We assume that $\{\!\{\chi^{(d)}_{\mathcal{F}\cup\{P_1^r,P_2^r\},G,v} \mid v \in V_G\}\!\} = \{\!\{\chi^{(d)}_{\mathcal{F}\cup\{P_1^r,P_2^r\},H,w} \mid w \in V_H\}\!\}$ implies $\chi^{(e)}_{\mathcal{F}\cup\{P^r\},G,v} = \chi^{(e)}_{\mathcal{F}\cup\{P^r\},H,w}$, and want to show that it also implies $\chi^{(e+1)}_{\mathcal{F}\cup\{P^r\},G,v} = \chi^{(e+1)}_{\mathcal{F}\cup\{P^r\},H,w}$. We again use the fact that we can associate with every $v \in V_G$ a unique vertex $w \in V_H$ such that $\chi^{(d)}_{\mathcal{F}\cup\{P_1^r,P_2^r\},G,v} = \chi^{(d)}_{\mathcal{F}\cup\{P_1^r,P_2^r\},H,w}$. In particular, this implies that $\chi^{(e)}_{\mathcal{F}\cup\{P_1^r,P_2^r\},G,v} = \chi^{(e)}_{\mathcal{F}\cup\{P_1^r,P_2^r\},H,w}$ and $\chi^{(e+1)}_{\mathcal{F}\cup\{P_1^r,P_2^r\},G,v} = \chi^{(e+1)}_{\mathcal{F}\cup\{P_1^r,P_2^r\},H,w}$. From the definition of the -WL-test, it must also be the case that the multisets $\{\chi^{(e)}_{\mathcal{F}\cup\{P_1^r,P_2^r\},G,v'} \mid v' \in N_G(v)\}$ and $\{\chi^{(e)}_{\mathcal{F}\cup\{P_1^r,P_2^r\},H,w'} \mid v' \in N_H(w)\}$ must be equal as well, i.e., we can find a one-to-one corresponence between neighbors of v in G and neighbors of w in H that have the same label. From the induction hypothesis we then have that $\chi^{(e)}_{\mathcal{F}\cup\{P^r\},G,v} = \chi^{(e)}_{\mathcal{F}\cup\{P^r\},H,w}$ and also that the multisets $\{\chi^{(e)}_{\mathcal{F}\cup\{P^r\},G,v'} \mid v' \in N_G(v)\}$ and $\{\chi^{(e)}_{\mathcal{F}\cup\{P^r\},H,w'} \mid v' \in N_H(w)\}$ are equal, which implies, by the definition of the WL-test, that $\chi^{(e+1)}_{\mathcal{F}\cup\{P^r\},G,v} = \chi^{(e+1)}_{\mathcal{F}\cup\{P^r\},H,w}$, as was to be shown.

C.3 Proof of Theorem 4

We show that $\mathcal{F} \cup \{Q^r\}$-WL, where Q^r is pattern whose core has treewidth k, is more expressive than $\mathcal{F}$-WL if every pattern $P^r \in \mathcal{F}$ satisfies one of the following conditions: (i) P^r has treewidth $< k$; or (ii) P^r does not map homomorphically to Q^r.

Let $c(Q)^r$ to denote the (rooted) core of Q, in which the root of $c(Q)^r$ is any vertex which is the image of the root of Q^r in a homomorphism from Q^r to $c(Q)^r$. By assumption, $c(Q)^r$ has treewidth k.

Clearly, $\mathcal{F}$-WL is upper bounded by $\mathcal{F} \cup \{Q^r\}$-WL. Thus, all we need for the proof is to find two graphs that are indistinguishable by $\mathcal{F}$-WL but are in fact distinguished by $\mathcal{F} \cup \{Q^r\}$-WL.

Those two graphs are, in fact, the graphs G and H constructed for $c(Q)^r$ (of treewidth k) in the proof of Theorem 3. From that proof, we know that:

(a) $\mathsf{hom}(c(Q), G) = 0$ and $\mathsf{hom}(c(Q), H) \neq 0$; and
(b) $G \equiv_{\mathsf{C}^k} H$.

We note that (a) immediately implies that G and H can be distinguished by $\mathcal{F} \cup \{Q^r\}$-WL. In fact, they are distinguished in already by the initial labelling in round 0. We next show that G and H are indistinguishable by $\mathcal{F}$-WL.

Let us first present a small structural result that helps us deal with patterns in $\mathcal{F}$ satisfying the second condition of the Theorem.

Lemma 4. *If a rooted pattern P^r does not map homomorphically to Q^r, then* $\mathsf{hom}(P, G) = \mathsf{hom}(P, H) = 0$

Proof. We use the following property of graphs G and H, which can be directly observed from their construction (and was already noted in Atserias et al. [2007] and Bova and Chen [2019]). Define G^r and H^r by setting as their root any vertex (a_r, f), for a_r the root of $c(Q)^r$. Then there is a homomorphism from G^r to $c(Q)^r$, and there is a homomorphism from H^r to $c(Q)^r$.

Now, any homomorphism h from P^r to G can be extended to a homomorphism from P^r to Q^r: we compose h with the homomorphism mentioned above from G to $c(Q)^r$, which by definition again maps homomorphically to Q^r. Since by definition we have that P^r does not map to Q^r, h cannot exist. The proof for H is analogous. □

Now, let $\mathcal{F}'$ be the set of patterns obtained by removing from $\mathcal{F}$ all patterns which do not map homomorphically to Q^r. By Lemma 4, we have that G and H are distinguished by the $\mathcal{F}$-WL-test if and only if they are distinguished by $\mathcal{F}'$-WL.

But all patterns in $\mathcal{F}'$ must have treewidth less than k, and by (b) G and H are indistinguishable by k-WL. Proposition 3 then implies that G and H are indistinguishable by $\mathcal{F}$-WL, as desired.

D Connections to existing formalisms

We here provide more details of how $\mathcal{F}$-MPNNs connect to MPNNs from the literature which also augment the initial labelling.

Vertex degrees. We first consider so-called *degree-aware* MPNNs Geerts et al. [2021] in which the message functions of the MPNNs may depend on the vertex degrees. The Graph Convolution Networks (GCNs) Kipf and Welling [2017] are an example of such MPNNs. Degree-aware MPNNs are known to be equivalent, in terms of expressive power, to standard MPNNs in which the initial labelling is extended with vertex degrees Geerts et al. [2021]. Translated to our setting, we can simply let $\mathcal{F} = \{\overset{\bullet}{\circ}\}$ since $\mathsf{hom}(\overset{\bullet}{\circ}, G^v)$ is equal to the degree of vertex v in G. When considering graphs without an initial vertex labelling (or a uniform labelling which assigns every vertex the same label), our characterisation (Theorem 1) implies $G \equiv^{(d)}_{\overset{\bullet}{\circ}\text{-WL}} H$ if and only if $\mathsf{hom}(T, G) = \mathsf{hom}(T, H)$ for every $\{\overset{\bullet}{\circ}\}$-pattern tree of depth at most d. This in turn is equivalent to $\mathsf{hom}(T, G) = \mathsf{hom}(T, H)$ for every (standard) tree of depth at most $d + 1$. Indeed, $\{\overset{\bullet}{\circ}\}$-pattern trees of depth at most d are simply trees of depth $d + 1$. Combining this with the characterisation of WL by Dvorak [2010] and Dell et al. [2018], we thus have for unlabelled graphs that $G \equiv^{(d)}_{\overset{\bullet}{\circ}\text{-WL}} H$ if and only if $G \equiv^{(d+1)}_{\text{WL}} H$. So, by considering $\mathcal{F} = \{\overset{\bullet}{\circ}\}$-MPNNs one gains one round of computation compared to considering standard MPNNs. To lift this to labeled graphs, instead of $\mathcal{F} = \{\overset{\bullet}{\circ}\}$ one has to include labeled versions of the single edge pattern, in order to count the number of neighbours of a specific label for each vertex. This is done, e.g., by Ishiguro et al. [2020], who use the WL labelling obtained after the first round to augment the initial vertex labelling. This corresponds indeed by adding $\mathsf{hom}(T^r, G^v)$ as feature for every labeled tree of depth one. This results in that $G \equiv^{(d)}_{\overset{\bullet}{\circ}\text{-WL}} H$ if and only if $G \equiv^{(d+1)}_{\text{WL}} H$ for labelled graphs.

Walk counts. The *Graph Feature Networks* by Chen et al. [2019a] can be regarded as a generalisation of the previous approach. Instead of simply adding vertex degrees, the number of walks of certain lengths emanating from vertices are added. Translated to our setting, this corresponds to considering $\{L_2, L_3, \ldots, L_\ell\}$-MPNNs, where L_ℓ denotes a rooted path of length ℓ. For unlabelled graphs, our characterisation (Theorem 1) implies that $G \equiv^{(d)}_{L_1,\ldots,L_\ell\text{-WL}} H$ is upper bounded by $G \equiv^{(d+\ell)}_{\text{WL}} H$, simply because every $\{L_2, L_3, \ldots, L_\ell\}$-pattern tree of depth d is a standard tree of depth at most $d + \ell$.

Cycles. Li et al. [2019] extend MPNNs by varying the notion of neighbourhood over which is aggregated. One particular instance corresponds to an aggregation of features, weighted by the number of cycles of a certain length in each vertex (see discussion at the end of Section 4 in Li et al. [2019]). Translated to our setting, this corresponds to considering $\{C_\ell\}$-MPNNs where C_ℓ denotes the cycle of length ℓ. As mentioned in the main body of the paper, these extend MPNNs and result in architectures bounded by 2-WL (Proposition 5). This is in line with Theorem 3 from Li et al. [2019] stating that their framework strictly extends MPNNs and thus 1-WL.

Isomorphism counts. Another, albeit similar, approach to add structural information to the initial labelling is taken in the paper *Graph Substructure Networks* by Bouritsas et al. [2020]. The idea there is to extend the initial features with information about how often a vertex v appears in a subgraph of G which is isomorphic to PMore precisely, Bouritsas et al. [2020] consider a connected unlabelled graph P as pattern and partition its vertex set V_P orbit-wise. That is, $V_P = \biguplus_{i=1}^{o_P} V_P^i$ where o_P denotes the number of orbits of P. Here, $v, v' \in V_P^i$ whenever there is an automorphism h in $\mathsf{Aut}(P)$ mapping v to v'. Next, they consider all distinct subgraphs $G_1, \ldots, G_k$ in G which are isomorphic to P, denoted by $P \cong G_j$ for $j \in [k]$. We write $P \cong_f G_j$ when $P \cong G_j$ using a specific isomorphism f. Then for each orbit partition $i \in [o_P]$ and vertex $v \in V$, they define:

$$\mathsf{iso}(P, G, v, i) = |\{G_j \cong P \mid v \in V_{G_j}, \text{and there exists an } f \text{ s.t. } G_j \cong_f P \text{ and } f(v) \in V_P^i, j \in [k]\}|.$$

That is, the number of subgraphs G_j in G that can be isomorphically mapped to P are counted, provided that this can be done by an isomorphism which maps vertex v in G_j (and thus G) to one of the vertices in the ith orbit partition V_P^i of the pattern. A similar notion is proposed for edges, which we will not consider here. Similar to our extended features, the initial features of each vertex v is then augmented with $\big(\mathsf{iso}(P, G^v, i) \mid P \in \mathcal{F}, i \in [o_P]\big)$ for some set $\mathcal{F}$ of patterns. Standard MPNNs are executed on these augmented initial features. We refer to Bouritsas et al. [2020] for more details.

We can view the above approach as an instance of our framework. Indeed, given a pattern P in $\mathcal{F}$, for each orbit partition, we replace P by a different rooted version P^{r_i}, where r_i is a vertex in V_P^i. Which vertex in the orbit under consideration is selected as root is not important (because they are equivalent by definition of orbit). We then see that the standard notion of subgraph isomorphism counting directly translates to the quantity used in Bouritsas et al. [2020]:

$$\mathsf{sub}(P^{r_i}, G^v) := \text{number of subgraphs in } G \text{ containing } v \text{, isomorphic to } P^{r_i} = \mathsf{iso}(P, G, v, i).$$

It thus remains to express $\mathsf{sub}(P^{r_i}, G^v)$ in terms of homomorphism counts. This, however, follows from Curticapean et al. [2017] in which it is shown that $\mathsf{iso}(P^{r_i}, G^v)$ can be computed by a linear combination of $\mathsf{hom}(Q^{r_i}, G^v)$ where Q^{r_i} ranges over all graphs on which P^{r_i} can be mapped by means of a surjective homomorphism. For a given P^{r_i}, the finite set of such patterns is called the *spasm* of P^{r_i} in Curticapean et al. [2017] and can be easily computed.

Proposition 2 now readily follows. Indeed, consider a $\mathcal{P}$-GSN and replace each $P \in \mathcal{P}$ by its rooted versions P^{r_i}, for $i \in [o_P]$. Let $\mathcal{P}^+$ be the resulting set of (rooted) patterns. Then, the results by Curticapean et al. [2017] imply that $\mathsf{sub}(P^{r_i}, G^v)$ can be computed in terms of $\mathsf{hom}(Q^r, G^v)$, where Q^r is a pattern in the spasm $\mathsf{s}(\mathcal{P}^+)$ of $\mathcal{P}^+$. As a consequence, the expressive power of $\mathcal{P}$-GSNs is bounded by the power of $\mathsf{s}(\mathcal{P}^+)$-MPNNs (and thus also by the power of $\mathsf{s}(\mathcal{P}^+)$-WL).

Conversely, given an $\mathcal{F}$-MPNN one can, again using results by Curticapean et al. [2017], define a set $\mathcal{F}^\star$ of patterns, such that the subgraph isomorphism counts of patterns in $\mathcal{F}^\star$ can be used to compute the homomorphism counts of patterns in $\mathcal{F}$. Here, the set $\mathcal{F}^\star$ consists of the extensions of patterns in $\mathcal{F}$. An extension of a graph is a supergraph over the same set of vertices. As a consequence, $\mathcal{F}$-MPNNs are upper bounded by $\mathcal{F}^\star$-GSNs. This is all in agreement with Curticapean et al. [2017] in which it is shown that homomorphism counts, subgraph isomorphism counts and other notions of pattern counts are all interchangeable. Nevertheless, by using homomorphism counts one can gracefully extend known results about WL and MPNNs, as we have shown in the paper, and add little overhead.

We conclude this section be a sketch of the proof of Theorem 2. We already observed that given a $\mathcal{P}$-GSN we can view it as an MPNN using rooted graph patterns $\mathcal{P}^+$. The difference now lies in that subgraph isomorphism counts rather than homomorphism counts are used. If we inspect, however, the proof of Theorem 1, then one sees that the two most important properties of homomorphism counts used are: (a) $\mathsf{hom}(P^r \star Q^r, G^v) = \mathsf{hom}(P^r, G^v) \cdot \mathsf{hom}(Q^r, G^v)$; and (b) if we consider a $\mathcal{P}^+$-tree T^r of depth d, then $\mathsf{hom}(T^r, G^v)$ decomposes in an expression using homomorphism counts of $\mathcal{P}^+$-trees of depth $d-1$. It is important to observe that these properties do not necessarily hold when replacing homomorphism counts by subgraph isomorphism counts, however. Nevertheless, they do hold for the revised notion of homomorphism defined in the main paper. Indeed, when considering $\mathsf{shom}(T^r, G^v)$ we treat the backbone tree of T^r differently from the patterns joined at its vertices. More precisely, we only count those mappings $h : V_T \to V_G$ such that h is a homomorphism on the backbone of T^r, whilst for the joined patterns at the backbone's vertices, we require local isomorphisms. Moreover, we require $h(P^r, G^u)$ to be isomorphic to P^r for every copy of P^r joined with a vertex t in the backbone of T^r. These conditions imply that the function shom satisfies properties (a) and (b) used in the proof of Theorem 1 and replacing hom by shom in the proof suffices to show Theorem 2.

E Additional experimental information

E.1 Experimental setup

One of the crucial questions when studying the effect of adding structural information to the initial vertex labels is whether these additional labels enhance the performance of graph neural networks. In order to reduce the effect of specific implementation details of GNNs and choice of hyper-parameters, we start from the GNN implementations and choices made in the benchmark by Dwivedi et al. [2020][6]. and only change the initial vertex labels, while leaving the GNNs themselves unchanged. This ensures that we only measure the effect of augmenting initial features with homomorphism counts. We will use the GNNs from the benchmark, without extended features, as our baselines. For the same reasons, we use datasets proposed in the benchmark for their ability to statistically separate the performance of GNNs. All other parameters are taken as in Dwivedi et al. [2020] and we refer to that paper for more details.

Selected GNNs Dwivedi et al. [2020] divide the benchmarked GNNs into two classes: the MPNNs and the "theoretically designed" WL-GNNs. The first class is found to perform stronger and train faster. Hence, we chose to include the five following MPNN models from the benchmark:

- Graph Attention Network (GAT) as described in Velickovic et al. [2018]
- Graph Convolutional Network (GCN) as described in Kipf and Welling [2017]
- GraphSage as described in Hamilton et al. [2017]
- Mixed Model Convolutional Networks (MoNet) as described in Monti et al. [2017]
- GatedGCN as described in Bresson and Laurent [2017].

For GatedGCN we used the version in which positional encoding Belkin and Niyogi [2003] is added to the vertex features, as it is empirically shown to be the strongest performing version of this model by for the selected datasets Dwivedi et al. [2020]. We denote this version by $\text{GatedGCN}_{E,PE}$, referring to the presence of edge features and this positional encoding. Details, background and a mathematical formalization of the message passing layers of these models can be found in the supplementary material of Dwivedi et al. [2020].

As explained in the experimental section of the main paper, we enhance the vertex features with the log-normalized counts of the chosen patterns in every vertex of every graph of every dataset. The first layers of some models of Dwivedi et al. [2020] are adapted to take in this variation in input size. All other layers where left identical to their original implementation as provided by Dwivedi et al. [2020].

Hardware, compute and resources All models for ZINC, PATTERN and COLLAB were trained on a GeForce GTX 1080 337 Ti GPU, for CLUSTER a Tesla V100-SXM3-32GB GPU was used. Tables 6, 9, 12 and 15 report the training times for all combination of models and additional feature set. A rough estimate of the CO_2 emissions based on the total computing times of reported experiments (2 074 hours GeForce GTX 1080, 372 hours Tesla V100-SXM3-32GB), the computing times of not-included experiments (1 037 hours GeForce GTX 1080, 181 hours Tesla V100-SXM3-32GB), the GPU types (GeForce GTX 1080, Tesla V100-SXM3-32GB) and the geographical location (undisclosed to preserve anonymity) of our cluster results in a carbon emission of 135 kg CO_2 equivalent. This estimation was conducted using the MachineLearning Impact calculator presented in Lacoste et al. [2019].

E.2 Graph learning tasks

We here report the full results of our experimental evaluation for graph regression (Section E.2.1), link prediction (Section E.2.2) and vertex classification (Section E.2.3) as considered in Dwivedi et al. [2020]. More precisely, a full listing of the patterns and combinations used and the obtained results for the test sets can be found in Tables 4, 7, 10 and 13. Average training time (in hours) and the number of epochs are reported in Tables 6, 9, 12 and 15. Finally, the total number of model parameters are reported in Tables 5, 8, 11 and 14. All averages and standard deviations are over 4 runs with different random seeds. The main take-aways from these results are included in the main paper.

E.2.1 Graph regression with the ZINC dataset

Just as in Dwivedi et al. [2020] we use a subset (12K) of ZINC molecular graphs (250K) dataset Irwin et al. [2012] to regress a molecular property known as the constrained solubility. For each molecular graph, the vertex features are the types of heavy atoms and the edge features are the types

[6] The original implementations can be found on https://github.com/graphdeeplearning/benchmarking-gnns

of bonds between them. The following are taken from Dwivedi et al. [2020]:
Splitting. ZINC has 10 000 train, 1 000 validation and 1 000 test graphs.
Training.[7] For the learning rate strategy, an initial learning rate is set to 5×10^{-5} , the reduce factor is 0.5, and the stopping learning rate is 1×10^{-6}, the patience value is 25 and the maximal training time is set to 12 hours.
Performance Measure The performance measure is the mean absolute error (MAE) between the predicted and the ground truth constrained solubility for each molecular graph.
Number of layers Most experiments are performed with 16 MPNN layers, following the best performers in the benchmark. We also report results using 4 MPNN layers.
Hidden feature size The hidden feature sizes are (for GAT, GCN, GraphSage, MoNet and GatedGCN respectively) 144, 145, 108, 90 and 70.

Table 4: Full results of the mean absolute error (predicted constrained solubility vs. the ground truth) for selected cycle combinations and GNNs on the ZINC data set. The top part of the table refers to experiments using 16 layers, the bottom part to experiments using 4 layers. In addition, in the last two rows of each part of the table we compare between homomorphism counts (hom) and subgraph isomorphism counts (iso).

Pattern set $\mathcal{F}$	GAT	GCN	GraphSage	MoNet	GatedGCN$_{E,PE}$
None	0,47±0,02	0,35±0,01	0,25±0,01	0,44±0,01	0,34±0,05
$\{C_3\}$	0,45±0,01	0,36±0,01	0,25±0,00	0,44±0,00	0,30±0,01
$\{C_4\}$	0,34±0,02	0,29±0,02	0,26±0,01	0,30±0,01	0,27±0,06
$\{C_5\}$	0,44±0,02	0,34±0,02	0,23±0,01	0,42±0,01	0,27±0,03
$\{C_6\}$	0,31±0,00	0,27±0,02	0,25±0,01	0,30±0,01	0,26±0,09
$\{C_3, C_4\}$	0,33±0,01	0,27±0,01	0,24±0,02	0,32±0,01	0,23±0,03
$\{C_5, C_6\}$	0,28±0,01	0,26±0,01	0,23±0,01	0,28±0,01	0,20±0,03
$\{C_4, C_5, C_6\}$	0,24±0,00	0,21±0,00	0,20±0,00	0,25±0,01	0,16±0,02
$\{C_3, C_4, C_5, C_6\}$	0,23±0,00	0,21±0,00	0,20±0,01	0,26±0,02	0,18±0,02
$\{C_3, \ldots, C_{10}\}$ (hom)	**0,22±0,01**	**0,20±0,00**	0,19±0,00	**0,2376±0,01**	**0,1352±0,01**
$\{C_3, \ldots, C_{10}\}$ (iso)	0,24±0,01	0,22±0,01	**0,16±0,01**	0,2408±0,01	0,1357 ± 0,01
None	0,48±0,01	0,46±0,00	0,36±0,01	0,45±0,00	0,26±0,03
$\{C_3, \ldots, C_{10}\}$ (hom)	**0,20±0,02**	0,25±0,02	0,19±0,01	**0,17±0,01**	0,13±0,01
$\{C_3, \ldots, C_{10}\}$ (iso)	0,21±0,00	**0,23±0,03**	**0,16±0,01**	0,19±0,01	**0,11±0,01**

E.2.2 Link Prediction with the Collab dataset

Another set used in Dwivedi et al. [2020] is COLLAB, a link prediction dataset proposed by the Open Graph Benchmark (OGB) Hu et al. [2020] corresponding to a collaboration network between approximately 235K scientists, indexed by Microsoft Academic Graph. Vertices represent scientists and edges denote collaborations between them. For vertex features, OGB provides 128-dimensional vectors, obtained by averaging the word embeddings of a scientist's papers. The year and number of co-authored papers in a given year are concatenated to form edge features. The graph can also be viewed as a dynamic multi-graph, since two vertices may have multiple temporal edges between if they collaborate over multiple years. The following are taken from Dwivedi et al. [2020]:

Splitting. We use the real-life training, validation and test edge splits provided by OGB. Specifically, they use collaborations until 2017 as training edges, those in 2018 as validation edges, and those in 2019 as test edges.
Training. All GNNs use the same learning rate strategy: an initial learning rate is set to 1×10^{-3} , the reduce factor is 0.5, the patience value is 10, and the stopping learning rate is 1×10^{-5} .
Performance Measure. We use the evaluator provided by OGB Hu et al. [2020], which aims to measure a model's ability to predict future collaboration relationships given past collaborations. Specifically, they rank each true collaboration among a set of 100 000 randomly-sampled negative collaborations, and count the ratio of positive edges that are ranked at K-place or above (Hits@K). The value $K = 50$ as this gives the best value for statistically separating the performance of GNNs.

[7] Here and in the next tasks we are using the parameters used in the code accompanying Dwivedi et al. [2020]. In the paper, slightly different parameters are used.

Table 5: Total model parameters for selected cycle combinations and GNNs on the ZINC data set. The top part of the table refers to experiments using 16 layers, the bottom part to experiments using 4 layers. In addition, in the last two rows of each part of the table we compare between homomorphism counts (hom) and subgraph isomorphism counts (iso).

Pattern set $\mathcal{F}$	GAT	GCN	GraphSage	MoNet	GatedGCN$_{E,PE}$
None	358 273	360 742	388 963	401 148	408 135
$\{C_3\}$	358 417	360 887	389 071	401 238	408 205
$\{C_4\}$	358 417	360 887	389 071	401 238	408 205
$\{C_5\}$	358 417	360 887	389 071	401 238	408 205
$\{C_6\}$	358 417	360 887	389 071	401 238	408 205
$\{C_3, C_4\}$	358 561	361 032	389 179	401 328	408 275
$\{C_5, C_6\}$	358 561	361 032	389 179	401 328	408 275
$\{C_4, C_5, C_6\}$	358 705	361 177	389 287	401 418	408 345
$\{C_3, C_4, C_5, C_6\}$	358 849	361 322	389 395	401 508	408 415
$\{C_3, \ldots, C_{10}\}$ (hom)	359 425	361 902	389 827	401 868	408 695
$\{C_3, \ldots, C_{10}\}$ (iso)	359 425	361 902	389 827	401 868	408 695
None	102529	103222	105139	106092	106575
$\{C_3, \ldots, C_{10}\}$ (hom)	103681	104382	106003	106812	107135
$\{C_3, \ldots, C_{10}\}$ (iso)	103681	104382	106003	106812	107135

Table 6: Average training time in hours and number of epochs for selected cycle combinations and GNNs on the ZINC data set. The top part of the table refers to experiments using 16 layers, the bottom part to experiments using 4 layers. In addition, in the last two rows of each part of the table we compare between homomorphism counts (hom) and subgraph isomorphism counts (iso).

Model:	GAT		GCN		GraphSage		MoNet		GatedGCN$_{E,PE}$	
Pattern set $\mathcal{F}$	Time	Epochs	Time	Epochs	Time	Epochs	Time	Epochs	Time	Epochs
None	2,40	377	10,99	463	2,46	420	1,53	345	12,08	136
$\{C_3\}$	2,88	444	12,03	363	2,03	500	0,91	298	12,07	148
$\{C_4\}$	2,30	351	11,36	324	2,31	396	1,70	382	12,06	139
$\{C_5\}$	2,42	375	12,03	333	1,70	444	1,06	370	12,06	202
$\{C_6\}$	2,40	369	9,98	421	2,58	446	1,25	288	12,08	136
$\{C_3, C_4\}$	2,98	461	12,03	332	2,56	458	1,41	321	12,09	132
$\{C_5, C_6\}$	2,76	422	12,04	319	2,67	464	1,53	356	12,06	137
$\{C_4, C_5, C_6\}$	2,45	381	10,13	419	1,67	463	1,04	382	12,04	229
$\{C_3, C_4, C_5, C_6\}$	2,65	408	10,38	420	2,09	503	1,26	364	12,08	135
$\{C_3, \ldots, C_{10}\}$ (hom)	2,65	428	12,03	350	2,76	478	1,48	363	12,06	175
$\{C_3, \ldots, C_{10}\}$ (iso)	2,78	497	11,72	419	2,63	547	1,58	440	11,62	148
None	0,32	158	2,14	201	0,26	171	0,28	184	5,47	223
$\{C_3, \ldots, C_{10}\}$ (hom)	0,33	166	2,35	190	0,16	164	0,36	207	5,80	210
$\{C_3, \ldots, C_{10}\}$ (iso)	0,26	176	1,66	182	0,20	186	0,31	222	5,06	272

Number of layers 3 MPNN layers are used for every model.
Hidden feature size The hidden feature sizes are (for GAT, GCN, GraphSage, MoNet and GatedGCN respectively) 57, 74, 38, 53 and 35.

E.2.3 Vertex classification with PATTERN and CLUSTER

Finally, also used in Dwivedi et al. [2020] are the PATTERN and CLUSTER graph data sets, generated with the Stochastic Block Model (SBM) Abbe [2018], which is widely used to model communities in social networks by modulating the intra- and extra-communities connections, thereby controlling the difficulty of the task. A SBM is a random graph which assigns communities to each vertex as follows: any two vertices are connected with probability p if they belong to the same community, or they are connected with probability q if they belong to different communities (the value of q acts as the noise level).

Table 7: Full Results (Hits @50) for all selected pattern combinations and GNNs on the COLLAB data set.

Pattern set $\mathcal{F}$	GAT	GCN	GraphSage	MoNet	GatedGCN$_{E,PE}$
None	50,32±0,55	51,36±1,30	49,81±1,56	50,33±0,68	51,00±2,54
$\{K_3\}$	**52,87±0,87**	53,57±0,89	50,18±1,38	51,10±0,38	**51,57±0,68**
$\{K_4\}$	51,33±1,42	52,84±1,32	**51,76±1,38**	51,13±1,60	49,43±1,85
$\{K_5\}$	52,41±0,89	**54,60±1,01**	50,94±1,30	**51,39±1,23**	50,31±1,59
$\{K_3, K_4\}$	52,68±1,82	53,49±1,35	50,88±1,73	50,97±0,68	51,36±0,92
$\{K_3, K_4, K_5\}$	51,81±1,17	54,32±1,02	49,94±0,23	51,01±1,00	51,11±1,06

Table 8: Total number of model parameters for all selected pattern combinations and GNNs on the COLLAB data set.

Pattern set $\mathcal{F}$	GAT	GCN	GraphSage	MoNet	GatedGCN$_{E,PE}$
None	25 992	40 479	39 751	26 487	27 440
$\{K_3\}$	26 049	40 553	39 804	26 525	27 475
$\{K_4\}$	26 049	40 553	39 804	26 525	27 475
$\{K_5\}$	26 049	40 553	39 804	26 525	27 475
$\{K_3, K_4\}$	26 106	40 627	39 857	26 563	27 510
$\{K_3, K_4, K_5\}$	26 163	40 701	39 910	26 601	27 545

Table 9: Average training times and number of epochs for all selected pattern combinations and GNNs on the COLLAB data set.

Model:	GAT		GCN		MoNet		GraphSage		GatedGCN$_{E,PE}$	
Pattern set $\mathcal{F}$	Time	#Epochs	Time	#Epochs	Time	#Epochs	Time	#Epochs	Time	#Epochs
None	0,81	167	0,85	141	1,62	190	12,05	115,67	2,22	167
$\{K_3\}$	0,67	165	0,90	153	1,70	184	12,10	67,00	2,48	186
$\{K_4\}$	1,06	188	0,95	160	2,16	188	12,04	113,50	1,26	188
$\{K_5\}$	0,50	167	1,13	165	1,04	193	12,05	124,00	1,82	174
$\{K_3, K_4\}$	1,20	189	0,86	128	2,15	189	12,05	113,25	1,51	183
$\{K_3, K_4, K_5\}$	0,44	149	0,90	134	0,98	186	12,05	124,00	1,84	177

For the PATTERN dataset, the goal of the vertex classification problem is the detection of a certain pattern P embedded in a larger graph G. The graphs in G consist of 5 communities with sizes randomly selected between $[5, 35]$. The parameters of the SBM for each community is $p = 0.5$, $q = 0.35$, and the vertex features in G are generated using a uniform random distribution with a vocabulary of size 3, i.e., $\{0, 1, 2\}$. Randomly, 100 patterns P composed of 20 vertices with intra-probability $p_P = 0.5$ and extra-probability $q_P = 0.5$ are generated (i.e., 50% of vertices in P are connected to G). The vertex features for P are also generated randomly using values in $\{0, 1, 2\}$. The graphs consist of 44-188 vertices. The output vertex labels have value 1 if the vertex belongs to P and value 0 belongs to G.

For the CLUSTER dataset, the goal of the vertex classification is the detection of which cluster a vertex belongs. Here, six SBM clusters are generated with sizes randomly selected between $[5, 35]$ and probabilities $p = 0.55$ and $q = 0.25$. The graphs consist of 40-190 vertices. Each vertex can take an initial feature value in range $\{0, 1, 2, \ldots, 6\}$. If the value is i then the vertex belongs to class $i - 1$. If the value is 0, then the class of the vertex is unknown and need to be inferred. There is only one labelled vertex that is randomly assigned to each community and most vertex features are set to 0. The output vertex labels are defined as the community/cluster class labels.

The following are taken from Dwivedi et al. [2020]:

Splitting The PATTERN dataset has $10\,000$ train, $2\,000$ validation and $2\,000$ test graphs. The CLUSTER dataset has $10\,000$ train, $1\,000$ validation and $1\,000$ test graphs. We save the generated splits and use the same sets in all models for fair comparison.

Training For all GNNs, an initial learning rate is set to 1×10^{-3}, the reduce factor is 0.5, the patience value is 10, and the stopping learning rate is 1×10^{-5} .
Performance measure The performance measure is the average vertex-level accuracy weighted with respect to the class sizes.
Number of layers 16 MPNN layers are used for every model, following the best performers in the benchmark. For the PATTERN dataset, we also report results using 4 MPNN layers.
Hidden feature size The hidden feature sizes are (for GAT, GCN, GraphSage, MoNet and GatedGCN respectively) 136, 146, 108, 90 and 70.

Table 10: Full results of the weighted accuracy for selected pattern combinations and GNNs on the CLUSTER data set.

Pattern set $\mathcal{F}$	GAT	GCN	MoNet	GraphSage	GatedGCN$_{E,PE}$
None	70,86±0,06	**70,64±0,39**	71,15±0,33	72,25±0,52	**74,28±0,15**
$\{K_3\}$	71,60±0,15	64,88±4,16	72,21±0,19	72,97±0,23	74,14±0,12
$\{K_4\}$	71,40±0,24	60,64±2,93	72,14±0,19	72,57±0,19	74,16±0,24
$\{K_5\}$	71,26±0,39	66,60±1,47	**72,34±0,09**	72,60±0,24	74,23±0,07
$\{K_3, K_4\}$	**71,80±0,28**	50,94±22,98	72,32±0,27	**73,03±0,25**	74,17±0,13
$\{K_3, K_4, K_5\}$	71,63±0,26	63,03±3,72	72,32±0,36	72,65±0,13	74,03±0,19

Table 11: Total number of model parameters for all selected pattern combinations and GNNs on the CLUSTER data set.

Pattern set $\mathcal{F}$	GAT	GCN	MoNet	GraphSage	GatedGCN$_{E,PE}$
None	395 396	362 849	399 373	386 835	406 755
$\{K_3\}$	395 396	362 849	399 373	386 835	406 755
$\{K_4\}$	395 548	362 995	399 463	386 943	406 825
$\{K_5\}$	395 700	363 141	399 553	387 051	406 895
$\{K_3, K_4\}$	395 700	363 141	399 553	387 051	406 895
$\{K_3, K_4, K_5\}$	396 004	363 433	399 733	387 267	407 035

Table 12: Training times (in hours) and number of epochs for all selected pattern combinations and GNNs on the CLUSTER data set.

Model:	GAT		GCN		MoNet		GraphSage		GatedGCN$_{E,PE}$	
Pattern set $\mathcal{F}$	Time	#Epochs	Time	#Epochs	Time	#Epochs	Time	#Epochs	Time	#Epochs
None	1,62	109	2,83	117	1,54	125	0,95	101	10,40	92
$\{K_3\}$	1,52	107	2,67	85	1,72	145	1,08	102	11,01	89
$\{K_4\}$	1,18	107	1,94	80	1,62	149	0,90	102	10,23	90
$\{K_5\}$	1,23	106	2,30	84	1,68	143	0,92	99	10,68	91
$\{K_3, K_4\}$	1,53	102	1,97	82	1,89	153	0,94	99	10,80	90
$\{K_3, K_4, K_5\}$	1,62	105	1,96	82	1,95	157	0,97	100	10,25	91

Table 13: Full results of the weighted accuracy for selected pattern combinations and GNNs on the PATTERN data set. The top part of the table refers to experiments using 16 layers, the bottom part to experiments using 4 layers.

Pattern set $\mathcal{F}$	GAT	GCN	MoNet	GraphSage	GatedGCN$_{E,PE}$
None	78,83±0,60	71,42±1,38	85,90±0,03	70,78±0,19	**86,15±0,08**
$\{K_3\}$	84,34±0,09	61,54±2,20	86,59±0,02	84,75±0,11	85,02±0,20
$\{K_4\}$	84,43±0,40	63,40±1,55	86,60±0,02	84,51±0,06	85,40±0,28
$\{K_5\}$	83,47±0,11	64,18±3,88	86,57±0,02	83,73±0,10	85,63±0,22
$\{K_3, K_4\}$	85,44±0,24	81,29±2,82	86,58±0,02	85,85±0,13	85,80±0,20
$\{K_3, K_4, K_5\}$	**85,50±0,23**	**82,49±0,48**	**86,63±0,03**	**85,88±0,15**	85,56±0,33
None	77,64±1,66	61,23±0,57	85,82±0,05	70,85±1,25	85,94±0,08
$\{K_3, K_4, K_5\}$	**86,54±0,07**	**83,89±0,81**	**86,63±0,03**	**86,50±0,05**	**85,98±0,11**

Table 14: Total number of model parameters for selected pattern combinations and GNNs on the PATTERN data set. The top part of the table refers to experiments using 16 layers, the bottom part to experiments using 4 layers.

Pattern set $\mathcal{F}$	GAT	GCN	MoNet	GraphSage	GatedGCN$_{E,PE}$
None	394 632	362 117	398 921	386 291	406 403
$\{K_3\}$	394 784	362 263	399 011	386 399	406 473
$\{K_4\}$	394 784	362 263	399 011	386 399	406 473
$\{K_5\}$	394 784	362 263	399 011	386 399	406 473
$\{K_3, K_4\}$	394 936	362 409	399 101	386 507	406 543
$\{K_3, K_4, K_5\}$	395 088	362 555	399 191	386 615	406 613
None	110088	101069	103865	102467	104843
$\{K_3, K_4, K_5\}$	110544	101507	104135	102791	105053

Table 15: Training times (in hours) and number of epochs for selected pattern combinations and GNNs on the PATTERN data set. The top part of the table refers to experiments using 16 layers, the bottom part to experiments using 4 layers.

Model:	GAT		GCN		MoNet		GraphSage		GatedGCN$_{E,PE}$	
Pattern set $\mathcal{F}$	Time	Epochs	Time	Epochs	Time	Epochs	Time	Epochs	Time	Epochs
None	1,96	87	3,41	102	1,68	116	0,77	103	10,32	101
$\{K_3\}$	0,97	97	2,58	80	1,42	107	0,69	105	9,12	95
$\{K_4\}$	0,90	90	2,68	80	1,46	106	0,67	95	9,47	94
$\{K_5\}$	0,89	95	2,36	80	1,26	100	0,58	98	9,14	99
$\{K_3, K_4\}$	2,11	91	3,62	98	1,68	108	0,86	97	9,50	87
$\{K_3, K_4, K_5\}$	1,02	91	3,26	94	1,48	109	0,76	102	8,84	88
None	0,86	156	1,95	98	0,82	169	0,61	122	3,40	89
$\{K_3, K_4, K_5\}$	0,57	102	1,78	97	0,44	92	0,66	105	2,80	89